

*Delamination and adhesive contact models
and their mathematical analysis
and numerical treatment*

Tomáš Roubíček, Martin Kružík, Jan Zeman

Preprint no. 2011-017



Research Team 1
Mathematical Institute of the Charles University
Sokolovská 83, 186 75 Praha 8
<http://ncmm.karlin.mff.cuni.cz/>

This is a preprint version of the Chapter 13 to be published in: *Mathematical Methods and Models in Composites* (Ed. V.Mantić), Imperial College Press (Vol.5 in series 'Comput. Experiment. Meth. in Structures'), ISBN 978-1-84816-784-1. The preprint and its maintaining in this preprint series is with a kind permission from the Publisher. The whole book's web page is <http://www.icpress.co.uk/engineering/p805.html>.

Delamination and adhesive contact models and their mathematical analysis and numerical treatment

TOMÁŠ ROUBÍČEK,^{1,2,3} MARTIN KRUŽÍK,^{†4} JAN ZEMAN⁵

Abstract

This chapter reviews mathematical approaches to inelastic processes on surfaces of elastic bodies. We mostly consider a quasistatic and rate-independent evolution at small strains and the concept of the so-called energetic solution. This concept is applied e.g. to brittle/elastic delamination, cohesive contact problems, and to delamination in various modes. Beside the theoretical treatment, numerical experiments are also presented. Finally, generalizations to dynamical and thermodynamical processes are outlined, together with extension to homogenization of composite materials with debonding phases.

Contents

1	Introduction	3
2	Concepts in quasistatic rate-independent evolution	5
3	Mathematical concepts to solve the system (6)	6
4	Quasistatic brittle delamination, Griffith concept	12
5	Elastic-brittle delamination	16
5.1	The model and its asymptotics to brittle delamination	16
5.2	Numerical implementation	17
5.3	Illustrative example	19
6	Various refinements and enhancements	21
6.1	Cohesive contacts	21
6.2	Delamination in modes I, II and mixed modes	23
6.3	Multi-threshold delamination	27
6.4	Combination with other inelastic processes	27
6.5	Dynamical adhesive contact in visco-elastic materials	28
6.6	Thermodynamics of adhesive contact	29
7	Conclusion and further application	30

1 Introduction

This Chapter is devoted to the formulation and mathematical and numerical treatment of inelastic processes on surfaces. Through this chapter with the exception of Sections 6.5 and 6.6, these inelastic processes are considered to be *quasistatic* (no inertia is taken into account), and *rate independent* (no internal time scale is considered). We will address

¹Mathematical Institute, Charles University, Sokolovská 83, CZ-186 75 Praha 8, Czech Republic.

²Institute of Thermomechanics of the ASCR, Dolejškova 5, CZ-182 00 Praha 8, Czech Republic.

³Institute of Information Theory and Automation of the ASCR, Pod vodárenskou věží 4, CZ-182 08 Praha 8, Czech Republic.

⁴Department of Physics, Faculty of Civil Engineering, Czech Technical University, Thákurova 7, CZ-166 29 Praha 6, Czech Republic.

⁵Department of Mechanics, Faculty of Civil Engineering, Czech Technical University, Thákurova 7, CZ-166 29 Praha 6, Czech Republic.

only small-strain models. Our general framework will solely be based on the hypothesis that the evolution is governed by a time-dependent Gibbs'-type *stored energy* functional \mathcal{E} (involving external loading) and a *dissipation potential* \mathcal{R} which, being degree-1 positively homogeneous, reflects the rate-independence of the process (i.e. invariance under any monotone re-scaling of time). Both functionals are defined on a suitable state space considered here in the form $\mathcal{U} \times \mathcal{Z}$. With only a small loss of generality, we assume that \mathcal{R} involves just z -component of a state $q = (u, z) \in \mathcal{U} \times \mathcal{Z}$. This distinguishes z as a “slow” variable, while u is a “fast” variable because its velocity is not controlled by any dissipation.

To introduce informally the concept of the energetic approach to such a class of rate-independent systems, we consider a uniform discretization of a fixed finite time interval $[0, T]$ with a fixed time step τ . Given the initial data $(u^0, z^0) := (u(0), z(0))$, the values of state variables at the k -th time level $(u_\tau^k, z_\tau^k) := (u_\tau(k\tau), z_\tau(k\tau))$ with $k = 1, 2, \dots, T/\tau$ follow from solution of the *incremental variational problem*

$$\left. \begin{array}{l} \text{minimize} \quad (u, z) \mapsto \mathcal{E}(k\tau, u, z) + \mathcal{R}(z - z_\tau^{k-1}) \\ \text{subject to} \quad (u, z) \in \mathcal{U} \times \mathcal{Z}. \end{array} \right\} \quad (1)$$

This energy minimization concept provides a unified approach to both continuum thermodynamics of inelastic solids, e.g. [39, 75], as well as to computational inelasticity [21, 73, 74]. In addition, rigorous mathematical theory has been established to study the time-continuous behavior of the problem (1) (corresponding to the limit $\tau \rightarrow 0$), see [32, 59, 60, 69] and Section 3 below.

As a prototypical application of the energetic framework to modeling of composite materials and structures, we now briefly introduce a simplified *elastic delamination model* (sometimes also called *debonding*) treated in more detail later in Section 5. Here, we restrict our attention to two elastic domains Ω_1 and Ω_2 , sharing an interface Γ_C . The structure is subjected to a time-dependent hard-device loading by a Dirichlet boundary condition imposed by displacements $w_D(t)$ acting at the part of external boundary Γ_D (with $u_D(t)$ denoting an extension of $w_D(t)$ to bodies Ω_1 and Ω_2).

In this context, $u + u_D$ is used to denote the *displacement field*. Moreover, we will work with an *internal variable* z (possibly vectorial) describing inelastic delamination processes on the boundary Γ_C . Various possibilities are presented in this Chapter. A simplest scenario works with a scalar-valued *delamination parameter* considered as a function of $x \in \Gamma_C$, with $z = 1$ and $z = 0$ corresponding to coherent and fully damaged interfacial point x , respectively. The time-independent set \mathcal{U} consists of the kinematically admissible displacements, satisfying the Dirichlet boundary conditions on Γ_D and frictionless contact conditions on Γ_C :

$$u = 0 \text{ on } \Gamma_D \quad \text{and} \quad \llbracket u \rrbracket_n \geq 0 \text{ on } \Gamma_C, \quad (2)$$

where $\llbracket u \rrbracket_n$ denotes the normal component of the displacement jump $\llbracket u \rrbracket$. Analogously, the set of admissible internal variables \mathcal{Z} is defined as

$$0 \leq z \leq 1 \text{ on } \Gamma_C. \quad (3)$$

Now, given admissible u and z , the stored energy functional reads

$$\mathcal{E}(t, u, z) := \sum_{i=1}^2 \int_{\Omega_i} \mathbb{C}^{(i)} e(u) : e\left(\frac{1}{2}u + u_D(t)\right) dx + \int_{\Gamma_C} \frac{z}{2} \mathbb{K} \llbracket u \rrbracket \cdot \llbracket u \rrbracket dS, \quad (4)$$

where $e(u)$ denotes the small strain tensor associated with displacement u , $\mathbb{C}^{(i)}$ stores the stiffness tensor of the i -th domain and \mathbb{K} is the elastic interfacial stiffness. The dissipation rate is defined as

$$\mathcal{R}(\dot{z}) := \begin{cases} \int_{\Gamma_C} a |\dot{z}| dS & \text{if } \dot{z} \leq 0 \text{ on } \Gamma_C, \\ \infty & \text{otherwise,} \end{cases} \quad (5)$$

with a denoting the fracture energy, representing the energy dissipated by the complete delamination. The value ∞ in (5) is used to ensure unidirectionality of the delamination phenomena, i.e. no healing of interface is admissible during the loading process. Sometimes only finitely-valued \mathcal{R} is considered, which means that *healing*, or also called *rebonding* is allowed, cf. e.g. [22, 87, 90]. Such models are, however, mathematically less difficult than (5) and their interpretation is rather limited (as the configuration possibly shifted after complete delamination has tendency to remember its initial state after healing), and will not be particularly addressed in this chapter.

After the energy functionals (4) and (5) have been specified, the tools and techniques presented in the remainder of this Chapter allow to study rigorously the delamination evolution, including theoretically-supported numerical simulations. Note that generality of the energetic framework allows to incorporate naturally more realistic interfacial constitutive laws and/or coupling the delamination phenomena with other inelastic properties such as plasticity, damage, or phase transformations. In addition, the energy functional (4) can easily be adapted to the setting of periodic homogenization theory, which makes the framework directly applicable to the analysis of e.g. fiber/matrix debonding in fibrous composites, see also Section 7 for a concrete example.

2 Concepts in quasistatic rate-independent evolution

Besides, we consider a Banach space⁶ $\mathcal{X} \supset \mathcal{Z}$ on which \mathcal{R} is defined having a domain with a nonempty interior and being coercive, and degree-1 homogeneous in the sense $\mathcal{R}(\lambda z) = \lambda \mathcal{R}(z)$ for any $\lambda \geq 0$. At least \mathcal{X} has to be a Banach space (to define the degree-1 homogeneity), but here also \mathcal{U} and \mathcal{Z} will always be Banach spaces.

Formally, for $\mathcal{E} : [0, T] \times \mathcal{U} \times \mathcal{Z} \rightarrow \mathbb{R} \cup \{\infty\}$ and $\mathcal{R} : \mathcal{Z} \rightarrow [0, \infty]$, the rate-independent evolution we have in mind is governed by the following system of *doubly nonlinear degenerate parabolic/elliptic variational inclusions*:

$$\partial_u \mathcal{E}(t, u, z) \ni 0 \quad \text{and} \quad \partial \mathcal{R}(\dot{z}) + \partial_z \mathcal{E}(t, u, z) \ni 0, \quad (6)$$

where $\dot{z} := \frac{dz}{dt}$ and the symbol “ ∂ ” refers to a (partial) subdifferential,⁷ relying on that $\mathcal{R}(\cdot)$, $\mathcal{E}(t, \cdot, z)$, and $\mathcal{E}(t, u, \cdot)$ are convex functionals in all specific models considered in this Chapter.

In mechanics, the concept of internal variables and the inclusion (6), sometimes also called Biot’s equation [8], is related with so-called generalized standard materials [40], cf. also [27] specifically for adhesive contacts. There are sound variational principles supporting the abstract model (6), although their applicability should not be overestimated.

The first inclusion in (6) expresses the *minimum-energy principle*, saying that, at any time t , the displacement u minimizes $u \mapsto \mathcal{E}(t, u, z(t))$.

Assuming for simplicity \mathcal{E} smooth and denoting the partial differentials by \mathcal{E}'_t , \mathcal{E}'_u , and \mathcal{E}'_z , one can postulate a so-called Lagrangian in the form

$$\begin{aligned} \mathcal{L}(t, u, z, \dot{z}) &:= \frac{d}{dt} \mathcal{E} + \mathcal{R} \\ &= \mathcal{E}'_t(t, u, z) + \langle \mathcal{E}'_u(t, u, z), \dot{u} \rangle + \langle \mathcal{E}'_z(t, u, z), \dot{z} \rangle + \mathcal{R}(\dot{z}) \\ &= \mathcal{E}'_t(t, u, z) + \langle \mathcal{E}'_z(t, u, z), \dot{z} \rangle + \mathcal{R}(\dot{z}), \end{aligned} \quad (7)$$

where we also used the first inclusion in (6). Then the second inclusion in (6) can be derived as the first-order optimality condition for

$$\dot{z} \mapsto \mathcal{L}(t, u, z, \dot{z}) \quad \text{is minimal for any time } t. \quad (8)$$

⁶A normed linear space which is complete is called a Banach space. Recall that a normed space X is complete if every Cauchy sequence in X converges to a limit in X .

⁷Let us recall that the subdifferential $\partial f(x)$ of a convex function $f : X \rightarrow \mathbb{R} \cup \{\infty\}$ at a point x is defined as the convex closed subset $\partial f(x) := \{x^* \in X^* ; \forall v \in X : f(x) + \langle x^*, v - x \rangle \leq f(v)\}$ of the dual space X^* ; standardly, $\langle \cdot, \cdot \rangle : X^* \times X \rightarrow \mathbb{R}$ denotes the duality pairing between the Banach space X and its dual $X^* := \{x^* : X \rightarrow \mathbb{R}, \text{ linear and continuous}\}$.

One refers to (8) as a *minimum dissipation-potential principle*, cf. [21, 39, 73, 75].

The degree-1 homogeneity of \mathcal{R} still allows for further interpretation of the flow rule, i.e. the second inclusion in (6). Defining the convex “elastic domain” $K := \partial\mathcal{R}(0)$, the second inclusion in (6) means just $\langle \omega - \mathfrak{z}, w - \dot{z} \rangle \geq 0$ for any w and any $\omega \in \partial\mathcal{R}(w)$, where we introduced the so-called thermodynamical *driving force* $\mathfrak{z} \in -\partial_z \mathcal{E}(t, u, z)$. In particular, for $w = 0$ one obtains

$$\langle \mathfrak{z}, \dot{z} \rangle = \max_{\omega \in K} \langle \omega, \dot{z} \rangle . \quad (9)$$

To derive (9), we have used that $\mathfrak{z} \in \partial\mathcal{R}(\dot{z}) \subset \partial\mathcal{R}(0) = K$ thanks to the degree-1 homogeneity of $\mathcal{R}(\cdot)$, so that always $\langle \mathfrak{z}, \dot{z} \rangle \leq \max_{\omega \in K} \langle \omega, \dot{z} \rangle$. The identity (9) says that the dissipation due to the driving force \mathfrak{z} is maximal provided that the order-parameter rate \dot{z} is kept fixed, while the vector of possible driving stresses ω varies freely over all admissible driving stresses from K . This just resembles the so-called Hill’s *maximum-dissipation principle* [42], cf. also [51, 79, 91, 104].

Let us also remark that the set $K = \partial\mathcal{R}(0)$ determines \mathcal{R} because $\mathcal{R} = \delta_K^*$ with δ_K denoting the so-called indicator function⁸ of the set K and δ_K^* is its Legendre-Fenchel conjugate⁹. In terms of K , by standard convex-analysis calculus [30], (9) can also be written as

$$\dot{z} \in [\partial\delta_K^*]^{-1}(\mathfrak{z}) = \partial[[\delta_K^*]^*](\mathfrak{z}) = \partial\delta_K(\mathfrak{z}) = N_K(\mathfrak{z}) , \quad (10)$$

where $N_K(\mathfrak{z})$ denotes the normal cone¹⁰ to K at \mathfrak{z} . This is the principle well known from plasticity theory, saying that the rate of the internal parameter z (meaning, as a special case considered in plasticity theory, the plastic-deformation rate) belongs to the cone of outward normals to the elasticity domain, see also [51, 88] or [41, Sect.3.2], [55, Sect.2.4.4] or [89, Sect.2.6].

3 Mathematical concepts to solve the system (6)

To design the concept of a weak solution to (6), we use \mathfrak{z} as in Section 2, and use the definition to write the three subdifferentials in (6) as the system of three inequalities

$$\forall(t, \tilde{u}, \tilde{z}) : \quad \mathcal{R}(\tilde{z}) - \langle \mathfrak{z}(t), \tilde{z} - \dot{z}(t) \rangle \geq \mathcal{R}(\dot{z}(t)), \quad (11a)$$

$$\mathcal{E}(t, \tilde{u}, z(t)) \geq \mathcal{E}(t, u(t), z(t)), \quad (11b)$$

$$\mathcal{E}(t, u(t), \tilde{z}) + \langle \mathfrak{z}(t), \tilde{z} - z(t) \rangle \geq \mathcal{E}(t, u(t), z(t)) , \quad (11c)$$

where the first and third inequalities just say that $\mathfrak{z} \in \partial\mathcal{R}(\dot{z})$ and $-\mathfrak{z} \in \partial_z \mathcal{E}(t, u(t), z(t))$, respectively, while (11b) just says that $u(t)$ minimizes the energy $\mathcal{E}(t, \cdot, z(t))$. As \mathcal{R} is homogeneous only of degree 1, \dot{z} can be expected bounded only in the Bochner-Lebesgue space $L^1(0, T; \mathcal{X})$,¹¹ or rather even in the corresponding space of measures. Thus the expression $\langle \mathfrak{z}, \dot{z} \rangle$ in (11a) might not be well defined or not allow for a mathematical treatment as far as various limit procedures concerns. Thus it is desirable to substitute it. For this, we use the formal chain-rule

$$\begin{aligned} \mathcal{E}(T, u(T), z(T)) - \mathcal{E}(0, u_0, z_0) &= \int_0^T \frac{d}{dt} \mathcal{E}(t, u, z) dt \\ &= \int_0^T (\mathcal{E}'_t(t, u, z) - \langle \mathfrak{z}, \dot{z} \rangle) dt; \end{aligned} \quad (12)$$

⁸This means that $\delta_K(v) = 0$ if $v \in K$ and $\delta_K(v) = \infty$ if $v \notin K$.

⁹The Legendre-Fenchel conjugate $f^* : X^* \rightarrow \mathbb{R} \cup \{\infty\}$ of a function $f : X \rightarrow \mathbb{R} \cup \{\infty\}$ is defined as $f^*(x^*) := \sup_{x \in X} \langle x^*, x \rangle - f(x)$.

¹⁰Let us recall that the normal cone $N_K(x)$ to a convex set $K \subset X$ at $x \in X$ is defined as $N_K(x) := \{x^* \in X^* ; \forall v \in K : \langle x^*, v - x \rangle \leq 0\}$.

¹¹The notation $L^p(\cdot)$ stands for the Banach space of measurable functions whose p -power is integrable on the indicated domain, here $[0, T]$. Such spaces are called Lebesgue spaces. If the functions take values in a general Banach space \mathcal{X} , then one applies a natural generalization of measurability due to Bochner.

c.f. (7). We integrate (11a) over $[0, T]$ and substitute for $\int_0^T \mathcal{R}(\dot{z}) dt$ the total variation

$$\text{Diss}_{\mathcal{R}}(z, [0, T]) := \sup \sum_{j=1}^N \mathcal{R}(z(t_j) - z(t_{j-1})), \quad (13)$$

where the supremum is taken over all partitions $0 \leq t_0 < t_1 < \dots < t_{N-1} \leq t_N \leq T$ of $[0, T]$; indeed, if z is absolutely continuous, then $\text{Diss}_{\mathcal{R}}(z, [0, T]) = \int_0^T \mathcal{R}(\dot{z}) dt$. This turns (11a) into

$$\begin{aligned} \mathcal{E}(T, u(T), z(T)) + \text{Diss}_{\mathcal{R}}(z, [0, T]) - \int_0^T \mathcal{E}'_t(t, u, z) dt - \mathcal{E}(0, u_0, z_0) \\ \leq \int_0^T (\mathcal{R}(\tilde{z}) - \langle \mathfrak{z}, \tilde{z} \rangle) dt. \end{aligned} \quad (14)$$

Note that (14) implies the energy balance: more specifically, for $\tilde{z} = 0$ we get

$$\underbrace{\mathcal{E}(T, u(T), z(T))}_{\text{stored energy at time } t=T} + \underbrace{\text{Diss}_{\mathcal{R}}(z, [0, T])}_{\text{energy dissipated during } [0, T]} \leq \underbrace{\int_0^T \mathcal{E}'_t(t, u, z) dt}_{\text{work done by mechanical load}} + \underbrace{\mathcal{E}(0, u_0, z_0)}_{\text{stored energy at time } t=0}. \quad (15)$$

We will use the notation $B([0, T]; \mathcal{U})$ for the Banach space of bounded measurable functions $[0, T] \rightarrow \mathcal{U}$ defined everywhere, and $BV([0, T]; \mathcal{X})$ for functions $[0, T] \rightarrow \mathcal{X}$ with bounded variation¹²; recall that $\mathcal{X} \supset \mathcal{Z}$ is a Banach space on which \mathcal{R} is coercive, i.e. $\mathcal{R}(z) \geq \varepsilon \|z\|$ for some $\varepsilon > 0$.

Definition 3.1 (Weak solutions.) *The process $(u, z, \mathfrak{z}) : [0, T] \rightarrow \mathcal{U} \times \mathcal{Z} \times \mathcal{Z}^*$ is called a weak solution of the initial-value problem given by $(\mathcal{U} \times \mathcal{Z}, \mathcal{E}, \mathcal{R})$ and the initial condition (u_0, z_0) if $u \in B([0, T]; \mathcal{U})$, $z \in B([0, T]; \mathcal{Z}) \cap BV([0, T]; \mathcal{X})$, $\mathfrak{z} \in B([0, T]; \mathcal{Z}^*)$ and*

- (i) *the inequality (14) with (13) holds for any \tilde{z} smooth enough, so that (14) is well defined,*
- (ii) *(11b) holds for any $\tilde{u} \in \mathcal{U}$ and any $t \in [0, T]$,*
- (iii) *(11c) holds for any $\tilde{z} \in \mathcal{Z}$ and any $t \in [0, T]$,*
- (iv) *the initial conditions $u(0) = u_0$ and $z(0) = z_0$ hold.*

The advantage of the above definition is that it is completely derivative-free, i.e. no time derivative \dot{z} and no (sub)differentials of \mathcal{E} or \mathcal{R} occur explicitly in Definition 3.1. In fact, if $\mathcal{E}(t, \cdot, z)$ or $\mathcal{E}(t, u, \cdot)$ are not convex and thus (6) loses sense, Definition 3.1 still yields a certain generalized solution. If a weak solution (u, z, \mathfrak{z}) is such that \dot{z} is absolutely continuous (i.e. \dot{z} is not a measure but an L^1 -function) and if $\mathcal{E}(t, \cdot, z)$ and $\mathcal{E}(t, u, \cdot)$ are convex, then (u, z) solves the original problem (6) for a.e. time $t \in [0, T]$. This justifies the above definition.

A certain drawback of the above definition is rather low selectivity.¹³ A certain inconvenience is also the involvement of the driving-force field \mathfrak{z} valued in \mathcal{Z}^* , which obviously does not bear any generalization for spaces \mathcal{Z} 's lacking a linear structure, like the Griffith-delamination problem (39)–(40) below. Thus one may be tempted for further generalizations. As \mathcal{R} is degree-1 homogeneous and convex, it holds $\partial \mathcal{R}(\dot{z}) \subset \partial \mathcal{R}(0)$ and thus $-\mathcal{E}'_z(t, u, z) \in \partial \mathcal{R}(\dot{z})$ implies $\mathcal{R}(\tilde{z}) + \langle \mathcal{E}'_z(t, u, z), \tilde{z} \rangle \geq \mathcal{R}(0) = 0$. Convexity of $\mathcal{E}(t, \cdot, \cdot)$ and $\langle \mathcal{E}'_u(t, u, z), \tilde{u} \rangle$ then further imply $\mathcal{R}(\tilde{z}) + \mathcal{E}(t, \tilde{u} + u, \tilde{z} + z) - \mathcal{E}(t, u, z) \geq 0$, which is obviously just (16) below. Thus we arrive at the following:

¹²Recall that the variation of $z : [0, T] \rightarrow \mathcal{X}$ is defined as $\sup \sum_{j=1}^N \|z(t_j) - z(t_{j-1})\|$, where $\|\cdot\|$ is the norm on \mathcal{X} and the supremum is taken over all partitions of $[0, T]$.

¹³For example, weak solutions to the brittle delamination problem in the formulation (45) do not necessarily have the so-called Griffith property and do not recover the original problem (39)–(40) through the formula (46), in contrast to the energetic solutions (see Definition 3.2) which enjoy this property.

Definition 3.2 (Energetic solutions, [68, 69, 70]) *The process $(u, z) : [0, T] \rightarrow \mathcal{U} \times \mathcal{Z}$ is called an energetic solution to the initial-value problem given by $(\mathcal{U} \times \mathcal{Z}, \mathcal{E}, \mathcal{R})$ and the initial condition (u_0, z_0) if $u \in B([0, T]; \mathcal{U})$, $z \in B([0, T]; \mathcal{Z}) \cap BV([0, T]; \mathcal{X})$, and*

- (i) *the energy inequality (15) holds,*
- (ii) *the following stability inequality holds for any $t \in [0, T]$:*

$$\forall(\tilde{u}, \tilde{z}) \in \mathcal{U} \times \mathcal{Z} : \quad \mathcal{E}(t, u, z) \leq \mathcal{E}(t, \tilde{u}, \tilde{z}) + \mathcal{R}(\tilde{z} - z), \quad (16)$$

- (iii) *the initial conditions $u(0) = u_0$ and $z(0) = z_0$ hold.*

In fact, any energetic solution satisfies (15) as an equality and thus, more standardly, the definition of energetic solutions employs rather the energy equality. If an energetic solution exists it is also a weak solution. Indeed, if (15) holds then (14) follows because $\mathcal{R} \geq 0$ and $\langle \mathfrak{z}, \tilde{z} \rangle \geq 0$ due to the fact that $0 \in \partial \mathcal{R}(0)$. Taking $\tilde{z} := z$ in (16) shows (11b). Finally, setting $\tilde{u} := u$ in (16) and exploiting the convexity of $\mathcal{E}(t, u, \cdot)$ proves (11c).

An important step is to make a generalization of Definition 3.2 for $\mathcal{E}(t, \cdot, \cdot)$ nonconvex, which will just be a typical situation in the modeling of quasistatic delamination processes. Roughly speaking, energetic solutions tempt to evolve as soon as it is energetically not disadvantageous. It should be note that this may, however, not be exactly always in full agreement with response of real systems where some other rate-dependent phenomena may come into play at some occasions. For this reason, there are also some other concepts of solutions that are sometimes applicable and successfully competing with energetic solutions, cf. also [60] for a comparison with other concepts in general and [20, 45, 46, 47, 72] in the context of crack propagation.

An efficient theoretical tool to prove existence of energetic solutions is by an *implicit time-discretization* of (6). Being constructive, it simultaneously suggests a conceptual numerical algorithm; cf. Remark 3.9 below. Considering, for simplicity, an equidistant partition of $[0, T]$ with a time-step $\tau > 0$, it formally leads to the recursive problem

$$\partial_u \mathcal{E}(k\tau, u_\tau^k, z_\tau^k) \ni 0 \quad \text{and} \quad \partial \mathcal{R}\left(\frac{z_\tau^k - z_\tau^{k-1}}{\tau}\right) + \partial_z \mathcal{E}(k\tau, u_\tau^k, z_\tau^k) \ni 0 \quad (17)$$

for $k = 1, 2, \dots, T/\tau$, starting from $u_\tau^0 = u_0$ and $z_\tau^0 = z_0$. Note that, in fact, $\partial \mathcal{R}$ is homogeneous of degree 0 so that the factor $1/\tau$ can be omitted. The potential structure of the problem allows for a conceptually constructive way to obtain some solution to (17), namely by solving the incremental global-minimization problem, defined earlier by (1). Note that (17), the time-discretized analog of (6), is in the position of the first-order optimality condition for any solution to (1). This is also called a *direct method* to solve (17), i.e. no approximate problem is, in principle, needed to ensure existence of a solution to (17), see e.g. [23]. Of course, if $\mathcal{E}(t, \cdot, \cdot)$ is not convex, as always in the delamination problems, (17) might admit also other solutions. Yet, (1) is fitted with the energetic-solution concept which, in turn, is well amenable to mathematical and numerical treatment. The following assertion uses quite minimal hypotheses:

Proposition 3.3 (Existence of time-discrete solutions) *If $\mathcal{E}(t, \cdot, \cdot)$ is lower semicontinuous and coercive¹⁴ on $\mathcal{U} \times \mathcal{Z}$ and also $\mathcal{R} \geq 0$ is lower semicontinuous, then the incremental problem (1) possesses a solution.*

Let us consider a solution $(u_\tau^k, z_\tau^k) \in \mathcal{U} \times \mathcal{Z}$ of the incremental problem (1) at the level k . Comparing the energy value of (1) at a solution in the time step k with the energy at arbitrary (\tilde{u}, \tilde{z}) , we obtain the discrete stability:

$$\begin{aligned} \mathcal{E}(k\tau, u_\tau^k, z_\tau^k) &\leq \mathcal{E}(k\tau, \tilde{u}, \tilde{z}) + \mathcal{R}(\tilde{z} - z_\tau^{k-1}) - \mathcal{R}(z_\tau^k - z_\tau^{k-1}) \\ &\leq \mathcal{E}(k\tau, \tilde{u}, \tilde{z}) + \mathcal{R}(\tilde{z} - z_\tau^k) \end{aligned} \quad (18)$$

¹⁴It essentially means that the sub-level sets of $\mathcal{E}(t, \cdot, \cdot)$, i.e. $\{(u, z) \in \mathcal{U} \times \mathcal{Z}; \mathcal{E}(t, u, z) \leq c\}$, are, for any $c \in \mathbb{R}$ which makes them nonempty, compact in some topology of $\mathcal{U} \times \mathcal{Z}$ which makes $\mathcal{E}(t, \cdot, \cdot)$ and $\mathcal{R}(\cdot)$ lower semicontinuous.

where we also used the degree-1 homogeneity and the convexity of \mathcal{R} which yields the triangle inequality $\mathcal{R}(\tilde{z}-z_\tau^{k-1}) \leq \mathcal{R}(z_\tau^k-z_\tau^{k-1}) + \mathcal{R}(\tilde{z}-z_\tau^k)$.

Comparing the energy value of a solution at the level k with that at a solution $(u_\tau^{k-1}, z_\tau^{k-1})$ of the incremental problem (1) at the level $k-1$ gives $\mathcal{E}(k\tau, u_\tau^k, z_\tau^k) + \mathcal{R}(z_\tau^k - z_\tau^{k-1}) \leq \mathcal{E}(k\tau, u_\tau^{k-1}, z_\tau^{k-1}) + \mathcal{R}(z_\tau^{k-1} - z_\tau^{k-1}) = \mathcal{E}(k\tau, u_\tau^{k-1}, z_\tau^{k-1})$, which yields an upper estimate of the energy balance in the k^{th} -step:

$$\begin{aligned} & \mathcal{E}(k\tau, u_\tau^k, z_\tau^k) + \mathcal{R}(z_\tau^k - z_\tau^{k-1}) - \mathcal{E}((k-1)\tau, u_\tau^{k-1}, z_\tau^{k-1}) \\ & \leq \mathcal{E}(k\tau, u_\tau^{k-1}, z_\tau^{k-1}) - \mathcal{E}((k-1)\tau, u_\tau^{k-1}, z_\tau^{k-1}) \\ & = \int_{(k-1)\tau}^{k\tau} \mathcal{E}'_t(t, u_\tau^{k-1}, z_\tau^{k-1}) dt. \end{aligned} \quad (19)$$

Eventually, writing the stability (18) at the level $k-1$ and testing it by $(\tilde{u}, \tilde{z}) = (u_\tau^k, z_\tau^k)$ gives a lower estimate of the energy balance in the k^{th} -step:

$$\begin{aligned} & \mathcal{E}(k\tau, u_\tau^k, z_\tau^k) + \mathcal{R}(z_\tau^k - z_\tau^{k-1}) - \mathcal{E}((k-1)\tau, u_\tau^{k-1}, z_\tau^{k-1}) = \mathcal{E}((k-1)\tau, u_\tau^k, z_\tau^k) \\ & + \int_{(k-1)\tau}^{k\tau} \mathcal{E}'_t(t, u_\tau^k, z_\tau^k) dt + \mathcal{R}(z_\tau^k - z_\tau^{k-1}) - \mathcal{E}((k-1)\tau, u_\tau^{k-1}, z_\tau^{k-1}) \\ & \geq \int_{(k-1)\tau}^{k\tau} \mathcal{E}'_t(t, u_\tau^k, z_\tau^k) dt. \end{aligned} \quad (20)$$

It is convenient to introduce the notation for the piecewise constant interpolants \bar{u}_τ and \underline{u}_τ , defined by

$$\bar{u}_\tau(t) := u_\tau^k \quad \text{for } t \in ((k-1)\tau, k\tau], \quad (21a)$$

$$\underline{u}_\tau(t) := u_\tau^{k-1} \quad \text{for } t \in [(k-1)\tau, k\tau). \quad (21b)$$

The notation \bar{z}_τ and \underline{z}_τ has an analogous meaning. Besides, we define

$$\bar{\mathcal{E}}_\tau(t, u, z) := \mathcal{E}(k\tau, u, z) \quad \text{for } t \in ((k-1)\tau, k\tau]. \quad (21c)$$

In terms of these interpolants, one can write (18), (19), and (20) summed over k in a compact form (22)–(23):

Proposition 3.4 (Stability and two-sided energy estimate) *Let \mathcal{R} be degree-1 positively homogeneous and let $\mathcal{E}'_t(\cdot, u, z) \in L^1(0, T)$ for any (u, z) . Then the discrete stability*

$$\forall (\tilde{u}, \tilde{z}) \in \mathcal{U} \times \mathcal{Z} : \quad \bar{\mathcal{E}}_\tau(t, \bar{u}_\tau(t), \bar{z}_\tau(t)) \leq \bar{\mathcal{E}}_\tau(t, \tilde{u}, \tilde{z}) + \mathcal{R}(\tilde{z} - \bar{z}_\tau(t)) \quad (22)$$

holds for any $t \in [0, T]$, and, for any $s = k\tau \in [0, T]$, $k \in \mathbb{N}$, the following two-sided energy inequality holds:

$$\begin{aligned} & \int_0^s \mathcal{E}'_t(t, \bar{u}_\tau(t), \bar{z}_\tau(t)) dt \\ & \leq \bar{\mathcal{E}}_\tau(s, \bar{u}_\tau(s), \bar{z}_\tau(s)) + \text{Diss}_{\mathcal{R}}(\bar{z}_\tau, [0, s]) - \bar{\mathcal{E}}_\tau(0, u_0, z_0) \\ & \leq \int_0^s \mathcal{E}'_t(t, \underline{u}_\tau(t), \underline{z}_\tau(t)) dt. \end{aligned} \quad (23)$$

The two-sided energy estimate may facilitate the numerical solution of the global-optimization problem (1). It should be emphasized that in all the applications considered in Sections 4–6, the incremental problem (1) involves a nonconvex functional, whose minimization is therefore very delicate, and iterative procedures need good starting points. For this, various backtracking strategies just based on the two-sided energy estimate (23) have

been designed and tested in [5, 6, 67] for similar kinds of problems, see also Section 5.2 for additional details.

Let us assume, with certain restriction of generality but still covering all problems presented here, that:

$$\exists \epsilon > 0 \quad \forall t, u, z : \quad \mathcal{E}(t, u, z) \geq \epsilon(\|u\|_{\mathcal{U}}^2 + \|z\|_{\mathcal{Z}}^2) - 1/\epsilon, \quad (24a)$$

$$\exists \gamma \in L^1(0, T) \quad \forall t, u, z : \quad |\mathcal{E}'_t(t, u, z)| \leq \gamma(t)(1 + \|u\|_{\mathcal{U}}), \quad (24b)$$

$$\exists \epsilon > 0 \quad \forall z : \quad \mathcal{R}(z) \geq \epsilon\|z\|_{\mathcal{Z}}, \quad (24c)$$

Proposition 3.5 (Convergence of discrete solutions) *Let (24) hold, u_0 be stable, and $\mathcal{E}(t, \cdot, z)$ be strictly convex. For $\tau \rightarrow 0$, there is a subsequence of the sequence of approximate solutions $\{(\bar{u}_\tau, \bar{z}_\tau)\}_{\tau>0}$ which converges to some (u, z) in the sense*

$$\bar{u}_\tau(t) \rightarrow u(t) \text{ in } \mathcal{U} \quad \text{for any } t \in [0, T], \quad (25a)$$

$$\bar{z}_\tau(t) \rightarrow z(t) \text{ in } \mathcal{Z} \quad \text{for any } t \in [0, T], \quad (25b)$$

$$\text{Diss}_{\mathcal{R}}(\bar{z}_\tau, [0, t]) \rightarrow \text{Diss}_{\mathcal{R}}(z, [0, t]) \quad \text{for any } t \in [0, T], \quad (25c)$$

$$\mathcal{E}'_t(\cdot, \bar{u}_\tau(\cdot), \bar{z}_\tau(\cdot)) \rightarrow \mathcal{E}'_t(\cdot, u(\cdot), z(\cdot)) \quad \text{in } L^1(0, T). \quad (25d)$$

Moreover, every (u, z) obtained by such a limit process is an energetic solution to the problem $(\mathcal{E}, \mathcal{R}, z_0)$.

The proof of Proposition 3.5 standardly relies on the following steps:

- 1) a-priori estimates, derived from the upper energy estimate in (23) by using the coercivity/growth assumption (24) and Gronwall's inequality: namely one gets

$$\|\bar{u}_\tau\|_{\text{B}([0, T]; \mathcal{U})} \leq C, \quad (26a)$$

$$\|\bar{z}_\tau\|_{\text{B}([0, T]; \mathcal{Z}) \cap \text{BV}([0, T]; \mathcal{Z})} \leq C. \quad (26b)$$

- 2) selection of convergent subsequences by using Banach's and Helly's principles; the latter one is used for the z -component which has a bounded variation. Using additionally the strict convexity of $\mathcal{E}(t, \cdot, z)$, one shows that also the u -component converges at each time t .
- 3) passage to the limit in the discrete stability (22) by finding a so-called mutual recovery sequence [65], i.e.

$$\begin{aligned} \forall \text{ stable sequence}^{15} (t_k, u_k, z_k) \rightarrow (t, u, z) \quad \forall (\tilde{u}, \tilde{z}) \quad \exists (\tilde{u}_k, \tilde{z}_k) : \\ \limsup_{k \rightarrow \infty} (\mathcal{E}(t_k, \tilde{u}_k, \tilde{z}_k) + \mathcal{R}(\tilde{z}_k - z_k) - \mathcal{E}(t_k, u_k, z_k)) \\ \leq \mathcal{E}(t, \tilde{u}, \tilde{z}) + \mathcal{R}(\tilde{z} - z) - \mathcal{E}(t, u, z). \end{aligned} \quad (27)$$

- 4) passage to the limit by weak lower-semicontinuity in the upper energy estimate, i.e. in the second inequality in (23).

Merging Propositions 3.3 and 3.5, one obtains:

Corollary 3.6 (Existence of energetic solutions) *Under the assumptions of Propositions 3.3 and 3.5, energetic solutions in the sense of Definition 3.2 do exist.*

¹⁵A sequence $\{(t_k, u_k, z_k)\}_{k \in \mathbb{N}}$ is called stable if $\sup_{k \in \mathbb{N}} \mathcal{E}(t_k, u_k, z_k) < \infty$ and if $\mathcal{E}(t_k, u_k, z_k) \leq \mathcal{E}(t_k, \tilde{u}, \tilde{z}) + \mathcal{R}(\tilde{z} - z_k)$ for all $(\tilde{u}, \tilde{z}) \in \mathcal{U} \times \mathcal{Z}$.

Remark 3.7 (Special unidirectional processes) In a lot of models of delamination, \mathcal{R} has the special form

$$\mathcal{R}(\dot{z}) = \delta_K(\dot{z}) + \langle a, \dot{z} \rangle \quad (28)$$

with some cone $K \subset \mathcal{Z}$ and some $a \in \mathcal{Z}^*$ non-negative in the sense that $\langle a, z \rangle \geq 0$ for any $z \in K$. Then one can evaluate $\text{Diss}_{\mathcal{R}}(z, [0, T])$ in (14) very explicitly. Indeed, any solution satisfying (14) must have $\dot{z} \in K$, hence $z(t_j) - z(t_{j-1}) \in K$ for any $t_j \geq t_{j-1}$, so that (13) gives

$$\begin{aligned} \text{Diss}_{\mathcal{R}}(z, [0, T]) &= \sup \sum_{j=1}^N \langle a, z(t_j) - z(t_{j-1}) \rangle = \sup \langle a, z(t_N) - z(t_0) \rangle \\ &= \langle a, z(T) - z(0) \rangle = \mathcal{R}(z(T) - z(0)). \end{aligned} \quad (29)$$

In this particular case, one can equivalently consider the dissipation potential $\mathcal{R}_0 : \mathcal{Z} \rightarrow \{0, \infty\}$ as $\mathcal{R}_0(\dot{z}) = \delta_K(\dot{z})$, if one augments the stored energy by the term $\langle a, z \rangle$. In view of (6), this is obvious when writing

$$\begin{aligned} \partial \mathcal{R}(\dot{z}) + \partial_z \mathcal{E}(t, u, z) &= \partial[\mathcal{R}_0(\dot{z}) + \langle a, \dot{z} \rangle] + \partial_z \mathcal{E}(t, u, z) \\ &= \partial \mathcal{R}_0(\dot{z}) + a + \partial_z \mathcal{E}(t, u, z) = \partial \mathcal{R}_0(\dot{z}) + \partial_z \mathcal{E}_0(t, u, z) \end{aligned}$$

for $\mathcal{E}_0(t, u, z) := \mathcal{E}(t, u, z) + \langle a, z \rangle$. The philosophy behind this formula is that the contribution to the stored energy via a unidirectional process can never be gained back, and it is thus stored forever, which means that it is dissipated. This alternative setting has been considered, e.g., in [33, 76, 77, 78]. It should be emphasized that this purely mechanical alternative is no longer equivalent in the full thermodynamical context when the dissipated energy contributes to the heat production, in contrast to the stored energy, cf. Section 6.6.

Remark 3.8 (More general dissipation) Sometimes, it is useful to consider $\mathcal{R} = \mathcal{R}(u, z, \dot{z})$, and then the inclusion (6) modifies to

$$\partial_u \mathcal{E}(t, u, z) \ni 0, \quad \partial_z \mathcal{R}(u, z, \dot{z}) + \partial_z \mathcal{E}(t, u, z) \ni 0. \quad (30)$$

A-priori estimates based on the test by \dot{z} are the same. Now, in general, $\text{Diss}_{\mathcal{R}}(z; [0, T])$ in (15) depends also on the u -component and, in terms of a placeholder $q = (u, z)$, is defined by

$$\text{Diss}_{\mathcal{D}}(q; [0, T]) := \sup \sum_{i=1}^N \mathcal{D}(q(t_{i-1}, \cdot), q(t_i, \cdot)) \quad (31)$$

where the supremum is taken over all partitions of the type $0 \leq t_0 < t_1 < \dots < t_N \leq T$, $N \in \mathbb{N}$; here \mathcal{D} denotes a so-called *dissipation distance* defined in [58], reflecting the minimum dissipation-potential principle (8), by

$$\begin{aligned} \mathcal{D}(q_1, q_2) &:= \inf \left\{ \int_0^1 \mathcal{R}(u, z, \dot{z}) dt; \right. \\ &\quad \left. q = (u, z) \in C^1([0, 1]; \mathcal{X}), q(0) = q_1, q(1) = q_2 \right\}. \end{aligned} \quad (32)$$

Like before, one assumes the positive one-homogeneity of $\mathcal{R}(u, z, \cdot)$. This implies the triangle inequality

$$\forall q_1, q_2, q_3 \in \mathcal{U} \times \mathcal{Z} : \quad \mathcal{D}(q_1, q_3) \leq \mathcal{D}(q_1, q_2) + \mathcal{D}(q_2, q_3). \quad (33)$$

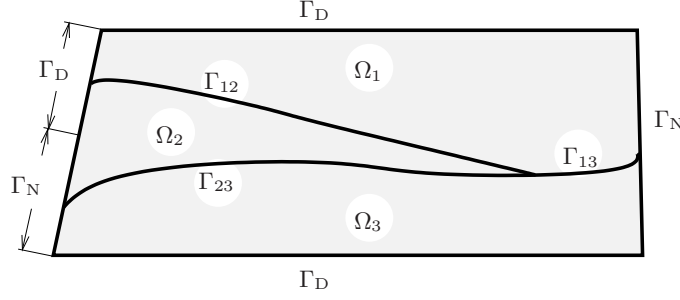


Figure 1: Illustration of the geometry and of the notation.

In terms of the dissipation distance, the incremental problem (1) takes the form

$$\left. \begin{array}{l} \text{minimize} \quad (u, z) \mapsto \mathcal{E}(k\tau, u, z) + \mathcal{D}((u_\tau^{k-1}, z_\tau^{k-1}), (u, z)) \\ \text{subject to} \quad (u, z) \in \mathcal{U} \times \mathcal{Z}. \end{array} \right\} \quad (34)$$

An important step to the conceptual generalization is to consider the dissipation distance $\mathcal{D} \geq 0$ satisfying (33) without any reference to \mathcal{R} , and even without requiring any linear structure on $\mathcal{U} \times \mathcal{Z}$. The mutual-recovery-sequence condition (27) then modifies as

$$\limsup_{k \rightarrow \infty} (\mathcal{E}(t_k, \tilde{q}_k) + \mathcal{D}(q_k, \tilde{q}_k) - \mathcal{E}(t_k, q_k)) \leq \mathcal{E}(t, \tilde{q}) + \mathcal{D}(q, \tilde{q}) - \mathcal{E}(t, q). \quad (35)$$

Note that, if $\mathcal{R} = \mathcal{R}(z)$ and \mathcal{Z} is a Banach space, formula (32) yields $\mathcal{D}(q_1, q_2) = \mathcal{R}(z_2 - z_1)$ with $q_i = (u_i, z_i)$, and one obtains the former case.

Remark 3.9 (Numerics) One can further approximate \mathcal{U} and \mathcal{Z} in (34) by some finite-dimensional Banach subspaces \mathcal{U}_h and \mathcal{Z}_h . Thus, in concrete situations, we obtain computationally implementable numerical strategies, as also demonstrated in Section 5.2. Besides, one has a convergence analysis for $h \rightarrow 0$ at one's disposal in specific cases; essentially, the proofs reduce to finding a suitable mutual-recovery-sequence for conditions similar to (27) or (35), but involving also a sequence of functionals \mathcal{E}_h which coincides with \mathcal{E} on $[0, T] \times \mathcal{U}_h \times \mathcal{Z}_h$ while being $= \infty$ elsewhere, cf. [64]. For an example see (51) below.

4 Quasistatic brittle delamination, Griffith concept

We shall now present models of quasistatic delamination that can be covered by the general abstract ansatz (6) or (30). We start, in this section, with models of brittle delamination.

Let $\Omega \subset \mathbb{R}^d$ ($d = 2, 3$) be a bounded Lipschitz domain¹⁶, and let us consider its decomposition into a finite number of mutually disjoint Lipschitz subdomains Ω_i , $i = 1, \dots, N$. Further denote $\Gamma_{ij} = \partial\Omega_i \cap \partial\Omega_j$ the (possibly empty) boundary between Ω_i and Ω_j . Thus, Γ_{ij} represents a prescribed $(d-1)$ -dimensional surface, which may undergo delamination. We assume that the boundary $\partial\Omega$ is the union of two disjoint subsets Γ_D and Γ_N , with

$$\mathcal{L}^{d-1}(\partial\Omega_i \cap \Gamma_D) > 0, \quad i = 1, \dots, N, \quad (36)$$

where \mathcal{L}^{d-1} denotes the $(d-1)$ -dimensional Lebesgue measure. On the Dirichlet part of the boundary Γ_D we impose a time-dependent boundary displacement $w_D(t)$, while the remaining part Γ_N is assumed to be free. Therefore, any admissible displacement $u : \cup_{i=1}^N \Omega_i \rightarrow \mathbb{R}^d$ has to be equal to a prescribed “hard-device” loading $w_D(t)$ on Γ_D .

¹⁶Recall that a domain is called Lipschitz if its boundary can be covered by a finite number of graphs of Lipschitz functions. Roughly speaking, it excludes corners of 0° or 360° angle, otherwise most domains considered in engineering are Lipschitz.

We consider here the case of linear elasticity determined, on each subdomain Ω_i , by the elastic-moduli tensor $\mathbb{C}^{(i)}$. Moreover, we take into account the local non-interpenetration of matter by requiring, for the displacement u , that $[[u]]_{ij} \cdot \nu_{ij} \geq 0$ on Γ_{ij} , where ν_{ij} denotes the unit normal to Γ_{ij} oriented from Ω_j to Ω_i . Here, $[[u]]_{ij}$ denotes the jump $u|_{\Omega_i} - u|_{\Omega_j}$, with $u|_{\Omega_i}$ being the trace on $\partial\Omega_i$ of the restriction of u to Ω_i . For

$$A \subset \Gamma_C := \bigcup_{i < j} \Gamma_{ij}, \quad (37)$$

we consider the stored-energy functional \mathcal{E} in the form

$$\mathcal{E}(t, u, A) := \begin{cases} \sum_{i=1}^N \frac{1}{2} \int_{\Omega_i} \mathbb{C}^{(i)} e(u) : e(u) \, dx & \text{if } u = w_D(t) \text{ on } \Gamma_D, \\ & [[u]]_n \geq 0 \text{ on } \Gamma_C, \\ & [[u(x)]] = 0 \text{ for } x \in A, \\ \infty & \text{elsewhere,} \end{cases} \quad (38)$$

where $e(u) = \frac{1}{2}(\nabla u)^\top + \frac{1}{2}\nabla u$ is the small-strain tensor, and where $[[u]]$ stands for the particular jump $[[u]]_{ij}$ on the whole union Γ_C of Γ_{ij} 's, and where we write shortly $[[u]]_n \geq 0$ on Γ_C instead of $[[u]]_{ij} \cdot \nu_{ij} \geq 0$ on Γ_{ij} , $i < j$. It means, in particular, that the part A of the contact boundary Γ_C is perfectly glued while the rest $\Gamma_C \setminus A$ is completely delaminated and a frictionless unilateral, so-called *Signorini contact* takes place there. This unilateral condition is important to prevent an unphysical delamination by a mere compression of the surface.

During the time-dependent loading w_D , the glued part $A = A(t)$ possibly evolves. In the simplest model, this process is considered unidirectional, i.e. healing is not allowed so that $t \mapsto A(t)$ is non-increasing, and for activation of delamination one needs (and thus dissipates) a specific energy $a : \Gamma_C \rightarrow \mathbb{R}^+$ (in Joule per area). The dissipated energy (understood also as the so-called dissipation distance) is then

$$\mathcal{D}(A_1, A_2) := \begin{cases} \int_{A_2 \setminus A_1} a(x) \, dS & \text{if } A_1 \subset A_2 \subset \Gamma_C, \\ \infty & \text{otherwise.} \end{cases} \quad (39)$$

In particular, the dissipated energy does not depend on particular fracture modes; cf. Section 6.2 below for a refinement of this model. The philosophy of such a quasistatic evolution is related with the *Griffith fracture criterion* [36], saying that the crack grows as soon as the energy release is bigger than the fracture toughness, here determined by a in (39). Such a sort of ‘‘geometrical’’ framework was used in the small-strain setting in [45, 72, 97] and in the large strains also in [47] for polyconvex materials¹⁷ and in [25] for quasiconvex materials¹⁸.

The definition of energetic solutions (15) involves time derivative of the stored energy, which is hardly defined for (38) unless w_D is constant in time. Therefore, using the additive shift $u - u_D(t)$ (where u_D is a suitable extension of the formerly defined w_D) we resort to constant Dirichlet boundary conditions. Thus, up to an irrelevant time-dependent constant, (38) transforms to

$$\mathcal{E}(t, u, A) := \begin{cases} \sum_{i=1}^N \int_{\Omega_i} \mathbb{C}^{(i)} e(u) : e\left(\frac{u}{2} + u_D(t)\right) \, dx & \text{if } u = 0 \text{ on } \Gamma_D, \\ & [[u]]_n \geq 0 \text{ on } \Gamma_C, \\ & [[u(x)]] = 0 \text{ for } x \in A, \\ \infty & \text{elsewhere,} \end{cases} \quad (40)$$

¹⁷Materials whose stored energy density is a convex function of the deformation gradient, its cofactor, and determinant.

¹⁸Materials whose stored energy density f is quasiconvex, i.e., $f(F)|\Omega| \leq \int_{\Omega} f(F + \nabla u(x)) \, dx$ for all smooth mappings $u : \Omega \rightarrow \mathbb{R}^3$ vanishing at $\partial\Omega$.

if one assumes that the Dirichlet loading allows for an extension such that

$$u_D|_{\Gamma_C} = w_D. \quad (41)$$

Note that, with a slight abuse of notation, the symbol u in (40) and thereafter denotes the shifted displacement field satisfying $u = 0$ on Γ_D . After such a shift of the Dirichlet boundary conditions, \mathcal{E}'_t does exist and one has the following simple formula for it:

$$\mathcal{E}'_t(t, u, A) = \sum_{i=1}^N \int_{\Omega_i} \mathbb{C}^{(i)} e(u) : e(\dot{u}_D(t)) \, dx. \quad (42)$$

Defining¹⁹

$$\mathcal{U} := \{u \in W^{1,2}(\Omega \setminus \Gamma_C; \mathbb{R}^d); u|_{\Gamma_D} = 0\}, \quad (43a)$$

$$\mathcal{Z} := \{A \subset \Gamma_C; A \text{ measurable}\} \quad (43b)$$

and adopting a generalization from Remark 3.8, one can claim:

Proposition 4.1 *Let $w_D \in W^{1,1}(I; W^{1/2,2}(\Gamma_D; \mathbb{R}^d))$ with $W^{1/2,2}$ denoting a Sobolev-Slobodetskii space²⁰ allow for an extension $u_D \in W^{1,1}(I; W^{1,2}(\Omega; \mathbb{R}^d))$ satisfying (41) and let $A_0 \subset \Gamma_C$ be measurable. Then the problem $(\mathcal{U} \times \mathcal{Z}, \mathcal{E}, \mathcal{D}, A_0)$ defined by (39), (40), and (43), possesses at least one energetic solution in the sense of Definition 3.2.*

Having such an energetic solution (u, A) , it is natural to consider the the shifted $(u+u_D, A)$ as a solution to the original problem with \mathcal{E} from (38) even if \mathcal{E}'_t is not well defined. Also, let us note that there is no explicit linear structure on A 's that would allow to write the first-order optimality conditions like (6) but, nevertheless, the concept of energetic solutions still works.

It is further convenient to reformulate this problem in a way that \mathcal{Z} will be a subset of a Banach space. For this, we introduce a so-called delamination parameter $z : \Gamma_C \rightarrow [0, 1]$, having the meaning of a fraction of fixed adhesive: $z(x) = 0$ means complete delamination and $z(x) = 1$ means 100% perfect bonding, while $z(x) = \frac{1}{2}$ means that 50% of the adhesive is debonded at $x \in \Gamma_C$ in question. Here it is appropriate to consider the model

$$\llbracket u(x) \rrbracket = 0 \text{ for a.a. } x \in \Gamma_C \text{ such that } z(x) > 0, \quad (44)$$

expressing that delamination can occur only if the adhesive is completely debonded, i.e. only if $z(x) = 0$. Thus, instead of (40), we now consider

$$\mathcal{E}(t, u, z) := \begin{cases} \sum_{i=1}^N \int_{\Omega_i} \mathbb{C}^{(i)} e(u) : e\left(\frac{u}{2} + u_D(t)\right) \, dx & \text{if } u = 0 \text{ on } \Gamma_D, \\ & \llbracket u \rrbracket_n \geq 0 \text{ on } \Gamma_C \\ & z \llbracket u \rrbracket = 0 \text{ on } \Gamma_C, \\ & 0 \leq z \leq 1 \text{ on } \Gamma_C, \\ \infty & \text{elsewhere,} \end{cases} \quad (45a)$$

the dissipation potential

$$\mathcal{R}(\dot{z}) := \begin{cases} \int_{\Gamma_C} a |\dot{z}| \, dS & \text{if } \dot{z} \leq 0 \text{ on } \Gamma_C, \\ \infty & \text{otherwise,} \end{cases} \quad (45b)$$

¹⁹Notation $W^{k,p}(\Omega)$ stands for the Banach space of functions on Ω whose k -th derivatives belong to L^p -space.

²⁰The space $W^{1/2,2}(\Gamma_D)$, involving fractional derivatives, is just the space of traces on Γ_D of all functions from $W^{1,2}(\Omega)$.

and, instead of (43b),

$$\mathcal{L} := L^\infty(\Gamma_C). \quad (45c)$$

Now we can use the concept of Definition 3.2:

Proposition 4.2 *Let $w_D \in W^{1,1}(I; W^{1/2,2}(\Gamma_D))$ and $0 \leq z_0 \leq 1$ be measurable. The problem $(\mathcal{U} \times \mathcal{L}, \mathcal{E}, \mathcal{R}, z_0)$ defined by (43a) and (45) possesses energetic solutions in the sense of Definition 3.2.*

The relation between the previous “geometrical” concept used in Proposition 4.1 and this “functional” concept is that, if z takes values only 0 or 1, i.e. always $z = \chi_A$ for some $A \subset \Gamma_C$,²¹ then

$$\mathcal{D}(A_1, A_2) = \mathcal{R}(z_2 - z_1) \quad \text{with } z_1 = \chi_{A_1}, \quad z_2 = \chi_{A_2}. \quad (46)$$

It has been proved in [66] that any energetic solution (u, z) to the brittle delamination problem, whose existence was stated in Proposition 4.2, is of the Griffith type in the sense that z takes values only 0 or 1. Thus, in particular, Proposition 4.1 is proved if Proposition 4.2 is proved. The latter one essentially relies on the explicit construction of the *mutual recovery sequence* for condition (27) from [86], namely

$$\tilde{u}_k := u_k \quad \text{and} \quad \tilde{z}_k := \begin{cases} z_k \tilde{z}/z & \text{where } z > 0 \\ 0 & \text{where } z = 0. \end{cases} \quad (47)$$

Note that always $0 \leq \tilde{z}_k \leq z_k$ and, if one considers $u_k \rightarrow u$ weakly in $W^{1,2}(\Omega; \mathbb{R}^d)$ and $z_k \rightarrow z$ weakly* in $L^\infty(\Gamma_C; \mathbb{R}^d)$,²² then also $\tilde{u}_k \rightarrow \tilde{u}$ weakly and $\tilde{z}_k \rightarrow \tilde{z}$ weakly*.

As the adhesive does not exhibit any elastic response in model (38), we refer to it as a *brittle delamination*.

The classical formulation corresponding to (6) with \mathcal{E} from (45a) and \mathcal{R} from (45b) consists in the equilibrium of forces on each subdomain Ω_i and several *complementarity problems*. Using a simplified notation $\mathbb{C} = \mathbb{C}(x) = \mathbb{C}^{(i)}$ if $x \in \Omega_i$, at a current time t , we can write it as:

$$\operatorname{div} \sigma = 0, \quad \sigma = \mathbb{C}^{(i)} e(u), \quad \text{in } \Omega_i, \quad i = 1, \dots, N, \quad (48a)$$

$$u = w_D(t, \cdot) \quad \text{on } \Gamma_D, \quad (48b)$$

$$\sigma \nu = 0 \quad \text{on } \Gamma_N, \quad (48c)$$

$$\left. \begin{aligned} & \llbracket \sigma \rrbracket \nu = 0, \\ & \llbracket u \rrbracket_n \geq 0, \quad \sigma_n(u) \llbracket u \rrbracket_n = 0 \\ & \sigma_n(u) \leq 0 \quad \text{wherever } z(t, \cdot) = 0 \\ & z \llbracket u \rrbracket = 0 \\ & \dot{z} \leq 0, \quad \xi \leq a, \quad \dot{z}(\xi - a) = 0, \\ & \xi \in N_{[0,1]}(z) + \partial_z I(\llbracket u \rrbracket, z) \end{aligned} \right\} \quad \text{on } \Gamma_C, \quad (48d)$$

where $N_{[0,1]}(\cdot) : \mathbb{R} \rightrightarrows \mathbb{R}$ is the normal-cone mapping, I denotes the indicator function of the constraint $z \llbracket u \rrbracket = 0$, ξ is the driving “force” for the delamination, $\sigma \nu := \mathbb{C}^{(i)} e(u)|_\Gamma \nu$ is the traction stress on $\Gamma = \Gamma_C$ or $\Gamma = \Gamma_N$ adjacent to Ω_i . Moreover, its normal and tangential components on Γ_C are denoted with $\sigma_n(u) = (\sigma \nu) \cdot \nu$ and $\sigma_t(u) = \sigma \nu - ((\sigma \nu) \cdot \nu) \nu$, respectively, so that we have the decomposition $\sigma \nu = \sigma_n \nu + \sigma_t$. We remark that, since by our choice ν turns out to be the inner unit normal on Ω_1 , σ_n in (48d) is non-positive.

²¹Here χ_A denotes the characteristic function of a set A , i.e. $\chi_A(x) = 1$ if $x \in A$ while $\chi_A(x) = 0$ otherwise.

²²The adjective “weak*” refers to testing by functions from a so-called pre-dual space. Here, as $L^\infty(\Gamma_C; \mathbb{R}^d) = L^1(\Gamma_C; \mathbb{R}^d)^*$, the weak* $L^\infty(\Gamma_C; \mathbb{R}^d)$ -convergence means that $\lim_{k \rightarrow \infty} \int_{\Gamma_C} z_k \cdot \varphi \, dS = \int_{\Gamma_C} z \cdot \varphi \, dS$ for every $\varphi \in L^1(\Gamma_C; \mathbb{R}^d)$.

5 Elastic-brittle delamination

In contrast with the previous Section 4, one can consider that the adhesive shows certain elastic response, and then one speaks about *elastic-brittle delamination*.

5.1 The model and its asymptotics to brittle delamination

Assuming linear response of the adhesive, the modification of (45a) can be considered as

$$\mathcal{E}_{\mathbb{K}}(t, u, z) := \begin{cases} \sum_{i=1}^N \int_{\Omega_i} \mathbb{C}^{(i)} e(u) : e\left(\frac{u}{2} + u_D(t)\right) dx \\ \quad + \int_{\Gamma_C} \frac{1}{2} z \mathbb{K} \llbracket u \rrbracket \cdot \llbracket u \rrbracket dS & \text{if } u = 0 \text{ on } \Gamma_D, \\ & \llbracket u \rrbracket_n \geq 0 \text{ on } \Gamma_C, \\ & 0 \leq z \text{ on } \Gamma_C, \\ \infty & \text{elsewhere,} \end{cases} \quad (49)$$

with \mathbb{K} being a positive-definite matrix expressing elastic response of the adhesive. Note that the constraint $z \leq 1$ cannot be active if the initial condition z_0 satisfies it, therefore it is not explicitly involved in $\mathcal{E}_{\mathbb{K}}$.

The classical formulation corresponding to (6) with $\mathcal{E} = \mathcal{E}_{\mathbb{K}}$ from (49) and \mathcal{R} from (45b) consists in equilibrium of forces on each subdomain Ω_i and three complementarity problems on Γ_C , corresponding to the three subdifferentials occurring in the involved functionals $\mathcal{E}_{\mathbb{K}}$ and \mathcal{R} . Before making the shift of the Dirichlet conditions, it reads (ρ is the Lagrange multiplier to the constraint $z \geq 0$):

$$\operatorname{div} \sigma = 0, \quad \sigma = \mathbb{C}^{(i)} e(u), \quad \text{in } \Omega_i, \quad i = 1, \dots, N, \quad (50a)$$

$$u = w_D(t, \cdot) \quad \text{on } \Gamma_D, \quad (50b)$$

$$\sigma \nu = 0 \quad \text{on } \Gamma_N, \quad (50c)$$

$$\left. \begin{aligned} \llbracket \sigma \rrbracket \nu &= 0 \\ \sigma \nu + z \mathbb{K} \llbracket u \rrbracket &= 0 \\ \llbracket u \rrbracket_n \geq 0, \quad \sigma_n(u) \leq 0, \quad \sigma_n(u) \llbracket u \rrbracket_n &= 0 \\ \dot{z} \leq 0, \quad \frac{1}{2} \mathbb{K} \llbracket u \rrbracket \cdot \llbracket u \rrbracket + \rho &\leq a \\ \dot{z} \left(\frac{1}{2} \mathbb{K} \llbracket u \rrbracket \cdot \llbracket u \rrbracket + \rho - a \right) &= 0 \\ z \geq 0, \quad \rho \leq 0, \quad \rho z &= 0. \end{aligned} \right\} \quad \text{on } \Gamma_C, \quad (50d)$$

Mathematically speaking, the elastic-brittle delamination is in a position of a regularization of the mere brittle delamination. In fact, the condition $z \llbracket u \rrbracket = 0$ in (45a) can obviously be modified to $\sqrt{z} \llbracket u \rrbracket = 0$ with entirely the same effect, and then, after a penalization by using a quadratic penalty with an L^2 -type (possibly anisotropic) norm $(\int_{\Gamma_C} \mathbb{K} u \cdot u dS)^{1/2}$ yields exactly (49). Thus, one can expect convergence²³ for $\mathbb{K} \rightarrow \infty$ to the brittle delamination. This has actually been proved in [86].

For a computer implementation, one also needs a spatial discretization. The simplest choice is P1-finite elements for u , P0-finite elements for z , assuming that all Ω_i are polyhedral and triangulated consistently on the joint boundary Γ_C . The *mutual recovery sequence*, cf. Remark 3.9 above, can be taken as:

$$\tilde{u}_h := \Pi_{\mathcal{U},h} \tilde{u}, \quad \tilde{z}_h := z_h \Pi_{\mathcal{Z},h} (\tilde{z}/z) \quad (51)$$

where $\tilde{z}(x)/z(x)$ is defined 0 if $z(x) = 0$, where $h = 1/k$ denotes a mesh size and $\Pi_{\mathcal{U},h}$ and $\Pi_{\mathcal{Z},h}$ are standard projectors on the finite-element subspace, the latter one making

²³The shorthand notation $\mathbb{K} \rightarrow \infty$ means that the minimal eigenvalue of \mathbb{K} goes to ∞ .

element-wise constant averages.²⁴ Merging it with a time discretization, a general result follows [65]. If we consider P1-elements for z with $\Pi_{Z,h}$ the corresponding projector, we can take $\tilde{z}_h = \Pi_{Z,h}(\tilde{z} - \|z_h - z\|_{L^\infty(\Gamma_C)})^+$, where $^+$ denotes the positive part. Merging the convergence to the brittle limit $\mathbb{K} \rightarrow \infty$ with numerical approximation $(\tau, h) \rightarrow (0, 0)$ seems possible only in a rather implicit way, cf. also [4, 66] for such a sort of results.²⁵

Altogether, we can summarize:

Proposition 5.1 *Assume (43a) and (45c). Let $(u_{\mathbb{K}}, z_{\mathbb{K}})$ denote the energetic solution to the problem $(\mathcal{E}_{\mathbb{K}}, \mathcal{R})$ from (49) and (45b). Let $(u_{\mathbb{K},\tau}, z_{\mathbb{K},\tau})$ stand for the approximate solutions obtained by the implicit semi-discretization in time (with a time step τ), and $(u_{\mathbb{K},\tau,h}, z_{\mathbb{K},\tau,h})$ for its numerical approximation constructed by this implicit time discretization and the above described FEM-discretization in space (with h a mesh parameter). Let also the above qualification of w_D and z_0 be satisfied. Then:*

- (i) *If $\mathbb{K} \rightarrow \infty$, then $(u_{\mathbb{K}}, z_{\mathbb{K}})$ converges (in terms of subsequences) to energetic solutions to the brittle problem $(\mathcal{E}, \mathcal{R})$ from (45a) and (45b) in the sense (25). The same holds also for $(u_{\mathbb{K},\tau}, z_{\mathbb{K},\tau})$ for $\mathbb{K} \rightarrow \infty$ and $\tau \rightarrow 0$.*
- (ii) *For \mathbb{K} fixed and for $(\tau, h) \rightarrow (0, 0)$, $(u_{\mathbb{K},\tau,h}, z_{\mathbb{K},\tau,h})$ converges (in terms of subsequences) to energetic solutions to $(\mathcal{E}_{\mathbb{K}}, \mathcal{R})$.*
- (iii) *There is $H : \mathbb{R}^{d \times d} \rightarrow \mathbb{R}^+$ converging to 0 sufficiently fast for $\mathbb{K} \rightarrow \infty$ such that the “stability criterion” $h \leq H(\mathbb{K})$ ensures the convergence of $(u_{\mathbb{K},\tau,h}, z_{\mathbb{K},\tau,h})$ (in terms of subsequences) to energetic solutions to the brittle problem $(\mathcal{E}, \mathcal{R})$.*

5.2 Numerical implementation

The theoretical developments presented up to this point provide a convenient framework to an implementable numerical scheme by discretizing the time-incremental formulation (1) in the space variables by standard finite element methods, recall Remark 3.9. To this goal, each domain Ω_i is triangulated using elements with a mesh size h , cf. Remark 3.9 on page 12. Recall that we assume that the discretization is conforming, i.e. that two interfacial nodes belonging to the adjacent domains Ω_i and Ω_j are geometrically identical, and that the same mesh is used to approximate variables u and z . Note that, in what follows, we denote by boldface letters nodal discretized variables and omit the subscripts \mathbb{K} and h . Now, the finite element discretization with a suitable numbering of nodes yields a discrete incremental problem in the form

$$\left. \begin{array}{l} \text{minimize} \quad (\mathbf{u}, \mathbf{z}) \mapsto \mathcal{E}_h(k\tau, \mathbf{u}, \mathbf{z}) + \mathcal{R}_h(\mathbf{z} - \mathbf{z}_\tau^{k-1}) \\ \text{subject to} \quad \mathbf{B}_E \mathbf{u} = \mathbf{0}, \quad \mathbf{B}_I \mathbf{u} \geq \mathbf{0}, \quad \mathbf{z}_\tau^{k-1} \geq \mathbf{z} \geq \mathbf{0}. \end{array} \right\} \quad (52)$$

Here, $\mathbf{u} \in \mathbb{R}^{n_u}$ stores the nodal displacements for individual sub-domains and $\mathbf{z} \in \mathbb{R}^{n_z}$ designates the delamination parameters associated with interfacial element edges. The discretized stored energy functional receives the form, related to (49),

$$\mathcal{E}_h(t, \mathbf{u}, \mathbf{z}) = \mathbf{u}^\top \mathbf{K} \left(\frac{1}{2} \mathbf{u} + \mathbf{w}_D(t) \right) + \frac{1}{2} [\mathbf{u}]^\top \mathbf{k}(\mathbf{z}) [\mathbf{u}], \quad (53)$$

²⁴Note that the product of element-wise constant functions z_h and $\Pi_{\mathcal{X},h}(\tilde{z}/z)$ is again element-wise constant, hence $z_h \in \mathcal{Z}_h$. As $0 \leq \Pi_{\mathcal{X},h}(\tilde{z}/z) \leq 1$, we have also $0 \leq \tilde{z}_h \leq z_h$, hence $\mathcal{R}(\tilde{z}_h - z_h) < \infty$. As $\Pi_{\mathcal{X},h}(\tilde{z}/z) \rightarrow \tilde{z}/z$ in any $L^p(\Gamma_C)$, $p < +\infty$, and $z_h \rightarrow z$ weakly, from (51) we have $\tilde{z}_h \rightarrow z(\tilde{z}/z) = \tilde{z}$ weakly* in fact in $L^\infty(\Gamma_C)$ due to the a priori bound of values in $[0, 1]$.

²⁵More explicit H occurring in Proposition 5.1(iii) might be supported by local Lipschitz continuity of $(z, u) \mapsto z \llbracket u \rrbracket^2 : L^2(\Gamma_C) \times W^{1/2,2}(\Omega) \rightarrow L^1(\Gamma_C)$ and by a rate of approximation by FE discretisation in these norms, cf. [64, Prop.3.3]. If $d=3$, the mentioned continuity is due to $\|z_1 \llbracket u_1 \rrbracket^2 - z_2 \llbracket u_2 \rrbracket^2\|_{L^1(\Gamma_C)} \leq \|z_1 - z_2\|_{L^2(\Gamma_C)} \|\llbracket u_1 \rrbracket\|_{L^4(\Gamma_C)}^2 + 2\|z_2\|_{L^\infty(\Gamma_C)} (\|\llbracket u_1 \rrbracket\|_{L^4(\Gamma_C)} + \|\llbracket u_2 \rrbracket\|_{L^4(\Gamma_C)}) \|\llbracket u_1 - u_2 \rrbracket\|_{L^{4/3}(\Gamma_C)}$, and then due to the continuity of the trace operator $W^{1/2,2}(\Omega) \rightarrow L^2(\Gamma_C)$. To get a rate of convergence, it seems inevitable to use a gradient theory for z . Then $H(\mathbb{K}) \sim o(|\mathbb{K}|^{-1/2})$ is expected.

where $\mathbf{K} = \text{diag}(\mathbf{K}_1, \mathbf{K}_2, \dots, \mathbf{K}_N)$ is a symmetric positive semi-definite block-diagonal stiffness matrix of order n_u (derived from $\mathbb{C}^{(i)}$), $[\mathbf{u}] \in \mathbb{R}^{n_k}$ stores the displacement jumps at interfacial nodes, and \mathbf{k} is a symmetric positive-definite interfacial stiffness matrix of order n_k , which is derived from \mathbb{K} and depends linearly on \mathbf{z} . The discrete dissipation potential is expressed as

$$\mathcal{R}_h(\mathbf{z}) = -\mathbf{a}^\top \mathbf{z}, \quad (54)$$

where the entries of $\mathbf{a} \in \mathbb{R}^m$ store the amount of energy dissipated by the complete delamination of an interfacial element; see [49] for additional details. The constraints in problem (52) consist of the homogeneous Dirichlet boundary conditions prescribed at nodes specified by a full-rank $m_E \times n_u$ Boolean matrix \mathbf{B}_E , nodal non-penetration conditions specified by a full-rank matrix $\mathbf{B}_I \in \mathbb{R}^{m_I \times n_u}$ storing the corresponding components of the normal vector, and the box constraints on the internal variable.

The discrete incremental problem (52) represents a large-scale non-convex program (due to the $\mathbf{k}(\mathbf{z})$ -term), which is very difficult to be solved using a monolithic approach. Nevertheless, it can be observed that the problem is separately convex with respect to the variables \mathbf{u} and \mathbf{z} . This directly suggests the concept of the *alternating minimization* algorithm, proposed by Bourdin *et al.* [17] for variational models of fracture. In the current context, the algorithm is briefly summarized in Table 5.2.

Conceptual implementation of alternating minimization algorithm.

<ol style="list-style-type: none"> 1. Set $j = 0$ and $\mathbf{z}^{(0)} = \mathbf{z}_\tau^{k-1}$ 2. Repeat <ol style="list-style-type: none"> (a) Set $j = j + 1$ (b) Solve for $\mathbf{u}^{(j)}$: <div style="text-align: right; margin-top: 10px;"> $\left. \begin{array}{l} \text{minimize} \quad \mathbf{u} \mapsto \mathcal{E}_h(k\tau, \mathbf{u}, \mathbf{z}^{(j-1)}) \\ \text{subject to} \quad \mathbf{B}_E \mathbf{u} = \mathbf{w}_D(k\tau) \quad \mathbf{B}_I \mathbf{u} \geq \mathbf{0} \end{array} \right\} \quad (55)$ </div> (c) Solve for $\mathbf{z}^{(j)}$: <div style="text-align: right; margin-top: 10px;"> $\left. \begin{array}{l} \text{minimize} \quad \mathbf{z} \mapsto \mathcal{E}_h(k\tau, \mathbf{u}^{(j)}, \mathbf{z}) + \mathcal{R}_h(\mathbf{z} - \mathbf{z}_\tau^{k-1}) \\ \text{subject to} \quad \mathbf{z}_\tau^{k-1} \geq \mathbf{z} \geq \mathbf{0} \end{array} \right\} \quad (56)$ </div> (d) Until $\ \mathbf{z}^{(j)} - \mathbf{z}^{(j-1)}\ < \eta$ 3. Set $\mathbf{u}_\tau^k = \mathbf{u}^{(j)}$ and $\mathbf{z}_\tau^k = \mathbf{z}^{(j)}$

The individual sub-problems of the alternating minimization algorithm can efficiently be resolved using specialized solvers. In particular, step (55) now becomes a quadratic programming problem, for which optimal duality-based solvers have been recently developed [29, 28]. Owing to the piecewise constant approximation of the delamination parameters, problem (56) can be solved locally element-by-element in a closed form, see also [37, 38] for additional details.

Note that this method allows for non-constant $\mathbb{C}^{(i)}$ and works quite equally for non-homogeneous materials. Let us, however, mention that, if all $\mathbb{C}^{(i)}$ are independent of x , one can alternatively (and more efficiently) apply boundary-element methods (BEM); thus combining recent advances in BEM-based solvers for the Signorini problem [15] with developments in computational materials science [11, 34, 10, 35].

Even though the alternating minimization algorithm performs well for a wide range of computational examples, it only converges to a local minimizer of the objective function (52), cf. [16, 19], whereas the energetic solution concept relies on the global energy minimization. To overcome this discrepancy, Mielke *et al.* [67] proposed a heuristic *back-tracking algorithm* based on the two-sided energy inequality (23). The resulting algorithm proceeds as follows:

Conceptual implementation of energy-based backtracking-in-time procedure.

1. Set $k = 1$, $\mathbf{z}^0 = \mathbf{z}^{(0)} = \mathbf{1}$
2. Repeat
 - (a) Determine \mathbf{z}_τ^k using the alternating minimization algorithm for time t_k and initial value $\mathbf{z}^{(0)}$
 - (b) Set $\mathbf{z}^{(0)} = \mathbf{z}_\tau^k$
 - (c) If

$$\int_{t_\tau^{k-1}}^{t_\tau^k} \partial_t \mathcal{E}_h(t, \mathbf{u}_\tau^k, \mathbf{z}_\tau^k) dt \leq \mathcal{E}_h(t_k, \mathbf{u}_\tau^k, \mathbf{z}_\tau^k) + \mathcal{R}_h(\mathbf{z}_\tau^{k-1} - \mathbf{z}_\tau^k)$$

$$-\mathcal{E}_h(t_{k-1}, \mathbf{u}_\tau^{k-1}, \mathbf{z}_\tau^{k-1}) \leq \int_{t_\tau^{k-1}}^{t_\tau^k} \partial_t \mathcal{E}_h(t, \mathbf{u}_\tau^{k-1}, \mathbf{z}_\tau^{k-1}) dt,$$
 set $k = k + 1$
 - (d) Else set $k = k - 1$
 - (e) Until $k > T/\tau$

It should be noted that there is generally no guaranty that the algorithm will locate the global optimum of the objective function (52); nevertheless computational experiments suggest that it delivers solutions with lower energies than the basic alternating minimization scheme [16, 67]. An alternative approach is offered by stochastic optimization techniques [5, 6], but this comes at the expense of a substantial increase of computational cost.

5.3 Illustrative example

The basic features of the proposed numerical treatment will be demonstrated by means of the response of a two-layer beam subjected to flexure, imposed by a vertical displacement at the mid-span. The geometrical details of the experiment, adapted from [101], are shown on Figure 2; the thickness refers to a plane-stress model used in the calculations. The elastic properties of the bulk material are characterized²⁶ by the Young modulus 75 GPa and the Poisson ratio 0.3 (corresponding to aluminum), the interfacial fracture toughness is set to $a = 25 \text{ Jm}^{-2}$ and the maximum vertical displacement amounts to 1 mm at $T=1$. The problem is discretized by identical isosceles right triangles with side length h and uniform time step τ .

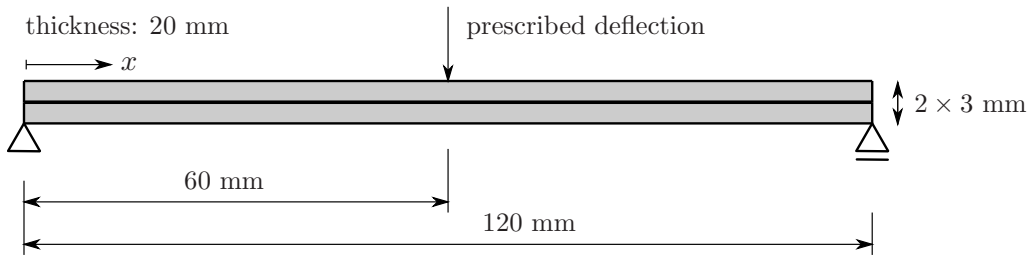


Figure 2: Setup of the flexure test.

The energetics of the delamination process is shown in Figure 3(a), highlighting the difference between the local energy minimization and the time back-tracking scheme. In particular, the local scheme predicts initially elastic behavior, followed by almost complete delamination of the two layers at $t \approx 0.56$, accompanied by the interfacial energy dissipation. However, exactly at this step the two-sided inequality is violated, as detected

²⁶This means we use an isotropic material with \mathbb{C} determined by $\mathbb{C}e:e = \lambda|\text{trace } e|^2 + 2\mu|e(u)|^2$ with the so-called Lamé constants $\lambda = \nu E / ((1+\nu)(1-2\nu))$ and $\mu = E / (2+2\nu)$, when E denotes the Young modulus and ν the Poisson ratio.

by the back-tracking algorithm. Inductively using such solution as the initial guess of the alternating iterative scheme, the algorithm returns to the original elastic path, thereby predicting a response leading to a lower value of the total energy for $t \in [0.46, 0.56]$. During the whole time interval, the contribution of the stored interfacial energy remains relatively small, owing to a large value of the interface stiffness. Notice that a small part of the interface remains intact even at $T = 1$, cf. Figure 3(b), due to the presence of compressive tractions at the mid-span. This explains why the dissipated energy in Figure 3(a) saturates at a slightly smaller value than 60 Nmm, which corresponds to the complete delamination.

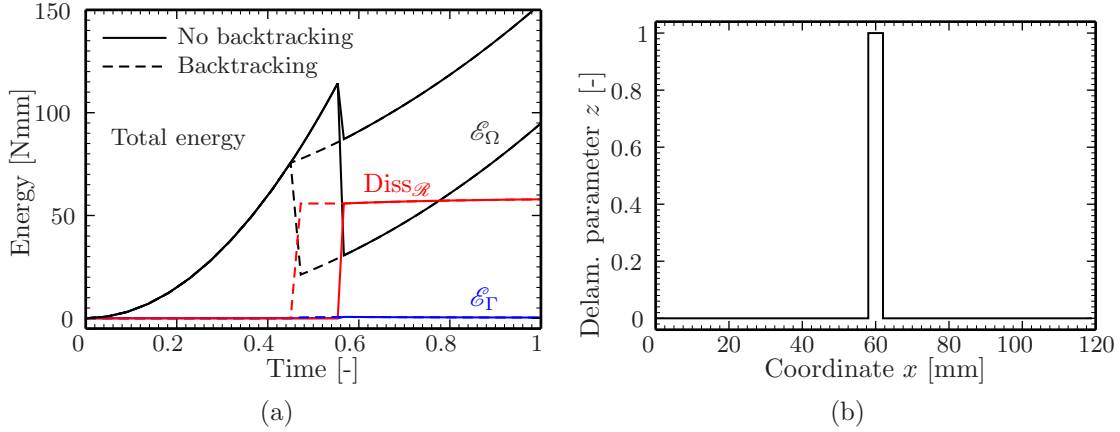


Figure 3: (a) Illustration of back-tracking procedure, (b) distribution of delamination parameter at $T = 1$; $h = 1$ mm, $\tau = 0.025$ and $\mathbb{K} = 10^5 \mathbb{I}$ GPa/m; \mathcal{E}_Ω = energy stored in bulk, \mathcal{E}_Γ = the interfacial contribution.

Figure 4 (a) demonstrates convergence of the approximate solutions for $h \rightarrow 0$. The results confirm that the overall energetic picture is almost independent of the spatial discretization, and that no spurious numerical oscillations are observed. The same conclusion holds for the force-displacement diagrams, shown in Figure 3(b).

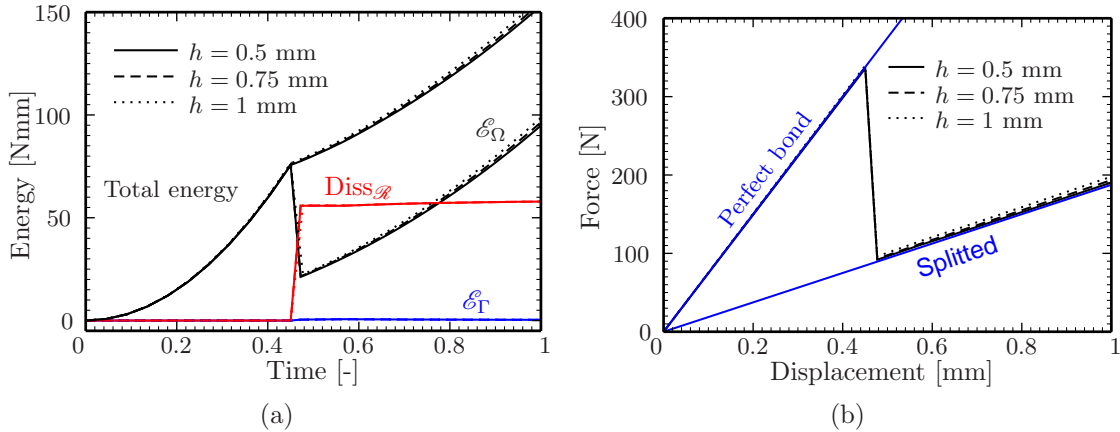


Figure 4: Convergence for $h \rightarrow 0$ for (a) energetics and (b) force-displacement diagram; $\tau = 0.025$ and $\mathbb{K} = 10^5 \mathbb{I}$ GPa/m; \mathcal{E}_Ω = energy stored in bulk, \mathcal{E}_Γ = the interfacial contribution.

Finally, the convergence of the debonding process as $\mathbb{K} \rightarrow \infty$ is illustrated in Figure 5. Notice that, similarly to the case $h \rightarrow 0$, the energetics appears to be only mildly dependent on the interfacial stiffness and that, already for $\mathbb{K} \approx 10^4 \mathbb{I}$ GPa/m, the FE-based solution accurately approximates the Griffith-type behavior discussed in Section 4.

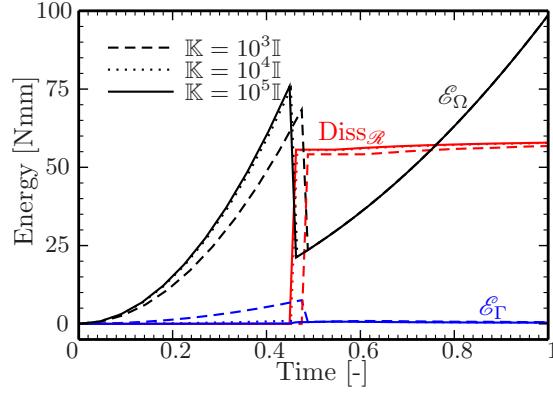


Figure 5: Convergence for $\mathbb{K} \rightarrow \infty$ towards the brittle model devised in [86]; $\tau = 0.025$ and $h = 0.5$ mm; \mathcal{E}_Ω = energy stored in bulk, \mathcal{E}_Γ = the interfacial contribution.

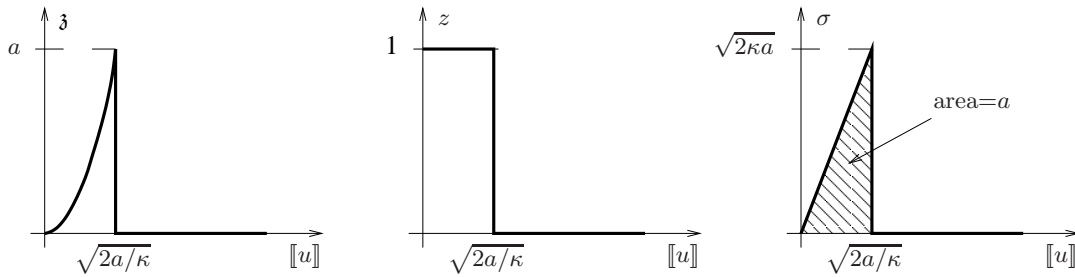


Figure 6: Schematic illustration of response of the driving force \mathfrak{z} , the delamination z , and the mechanical stress σ in model (49) with $\mathbb{K} = \kappa \mathbb{I}$ and (45b) under the displacement-controlled experiment.

6 Various refinements and enhancements

The models introduced so far represent rather a very basic scenario, which was intentionally simplified to make the explanation of the basic ideas easier. Engineers, however, deal with various advanced ideas not discussed yet. The goal of this section is to demonstrate that they can be involved in this theory, too.

6.1 Cohesive contacts

The adhesive model presented in Section 5 yields a discontinuous response of the mechanical stress $\sigma := \partial_{[u]}(\frac{z}{2}\mathbb{K}[u] \cdot [u]) = z\mathbb{K}[u]$ within a displacement-controlled experiment. Namely, starting from an unstressed configuration, the stress linearly increases with a prescribed $[u]$ until the driving force $\mathfrak{z} := \partial_z(\frac{z}{2}\mathbb{K}[u] \cdot [u]) = \frac{1}{2}\mathbb{K}[u] \cdot [u]$ reaches the activation threshold a used in (45b), then z jumps to zero and the mechanical stress jumps to zero, too; cf. Figure 6 depicted for the isotropic case $\mathbb{K} = \kappa \mathbb{I}$ with some $\kappa > 0$. Engineering literature often considers rather continuous response of the mechanical stress, however. It is referred to as a *cohesive-type contact* and urges some modification of the above model.

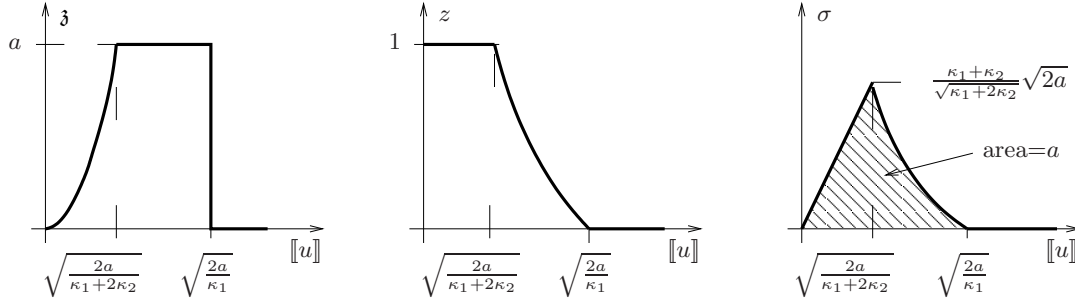


Figure 7: Schematic illustration of response of the refined model (57) with $\mathbb{K}_1 = \kappa_1 \mathbb{I}$ and $\mathbb{K}_2 = \kappa_2 \mathbb{I}$ and (45b) under the pulling experiment.

One simple option is to modify $\mathcal{E}_{\mathbb{K}}$ from (49) as follows

$$\mathcal{E}_{\mathbb{K}_1, \mathbb{K}_2}(t, u, z) := \begin{cases} \sum_{i=1}^N \int_{\Omega_i} \mathbb{C}^{(i)} e(u) : e\left(\frac{u}{2} + u_D(t)\right) dx \\ + \int_{\Gamma_C} \frac{z \mathbb{K}_1 \llbracket u \rrbracket + z^2 \mathbb{K}_2 \llbracket u \rrbracket}{2} \cdot \llbracket u \rrbracket \\ + \frac{\kappa_0}{r} |\nabla_s z|^r dS & \text{if } u = 0 \text{ on } \Gamma_D, \\ & \llbracket u \rrbracket_n \geq 0 \text{ on } \Gamma_C \\ & 0 \leq z \leq 1 \text{ on } \Gamma_C, \\ \infty & \text{elsewhere,} \end{cases} \quad (57)$$

where we used a $(d-1)$ -dimensional “surface” gradient²⁷ ∇_s and assume $r > d-1$ and, rather for mathematical reasons, $\kappa_0 > 0$. This last term has a similar “nonlocal” effect like in the frequently used gradient theory in damage; also the analysis and especially constructions of a mutual recovery sequence in the sense of [65] are the same as in damage models. In particular, for $1 < r \leq d-1$ one has to use a sophisticated construction from [95, 96], otherwise a simpler construction from [63] works, too. In the context of delamination, gradient theory has been used, e.g., in [33, Chap.14] or [12, 13].

To demonstrate the response of this model, let us confine ourselves to the isotropic adhesive response $\mathbb{K}_1 = \kappa_1 \mathbb{I}$ and $\mathbb{K}_2 = \kappa_2 \mathbb{I}$. Then, the mechanical stress $\sigma := \partial_{\llbracket u \rrbracket} \left(\frac{1}{2} (\kappa_1 z + \kappa_2 z^2) |\llbracket u \rrbracket|^2 \right) = (\kappa_1 z + \kappa_2 z^2) \llbracket u \rrbracket$ within a pulling experiment again linearly increases with $\llbracket u \rrbracket$ until the driving force $\mathfrak{z} := \partial_z \left(\frac{1}{2} (\kappa_1 z + \kappa_2 z^2) |\llbracket u \rrbracket|^2 \right) = \left(\frac{1}{2} \kappa_1 + \kappa_2 z \right) |\llbracket u \rrbracket|^2$ reaches a , which happens for $|\llbracket u \rrbracket| = \sqrt{2a / (\kappa_1 + 2\kappa_2)}$, and then z starts evolving while holding $\mathfrak{z} = a$, i.e. $z = \frac{a}{\kappa_2} |\llbracket u \rrbracket|^{-2} - \frac{\kappa_1}{2\kappa_2}$, until it arrives at 0, which happens for $|\llbracket u \rrbracket| = \sqrt{2a / \kappa_1}$; thus the mechanical stress decays as $\sigma = (\kappa_1 z + \kappa_2 z^2) \llbracket u \rrbracket = \left(\frac{a^2}{\kappa_2} |\llbracket u \rrbracket|^{-4} - \frac{\kappa_1^2}{4\kappa_2} \right) \llbracket u \rrbracket$ to zero, cf. Figure 7. The continuous response of σ (Fig.7-right) is addressed as a *cohesive-zone model*, cf. e.g. [98, 103]. Like (49), the feature of (57) is that it is separately quadratic both in the u - and the z -variable, so one can advantageously use alternating minimization algorithms to solve the incremental minimization problems of the type (1) as in [17, 19, 67].

More generally, one can consider a continuous, increasing function $\phi : [0, 1] \rightarrow \mathbb{R}^+$ with $\phi(0) = 0$, and replace the z -term under the surface integral in (49) by $\phi(z) |\llbracket u \rrbracket|^2$. Repeating the previous arguments, the response on the tensile experiment starting from $z = 1$ exhibits a quadratic dependence on the driving force $\mathfrak{z} = \phi'(z) |\llbracket u \rrbracket|^2$ until it reaches the activation threshold a , which happens for $|\llbracket u \rrbracket| = \sqrt{a / \phi'(1)}$. Then z starts evolving while holding $\mathfrak{z} = a$, which yields $z = [\phi']^{-1} (|\llbracket u \rrbracket|^2 / a)$ and the actual stress $\sigma = 2\phi([\phi']^{-1} (|\llbracket u \rrbracket|^2 / a)) \llbracket u \rrbracket$, until it arrives at 0.

Up to the gradient term, the equivalent effect can be obtained by a substitution of $\phi(z)$ by a new delamination variable, say ζ . It would lead to the stored-energy term $\zeta |\llbracket u \rrbracket|^2$ and

²⁷The notation $\nabla_s z$ of the surface gradient stands for $\nabla z - \nu(\nu \cdot \nabla z)$.

the dissipation distance $a|\phi^{-1}(\tilde{\zeta}) - \phi^{-1}(\zeta)|$ if $\tilde{\zeta} \leq \zeta$, which corresponds to the dissipation metric $a|\dot{\zeta}|/\phi'(\phi^{-1}(\zeta))$. Thus, in terms of this new variable, we obtain the situation

$$\text{effective activation} = \frac{a}{\phi'(\phi^{-1}(\zeta))}, \quad \text{stress} = 2\zeta \llbracket u \rrbracket. \quad (58)$$

while the driving force is $\llbracket u \rrbracket^2$. In fact, having an “optically” *non-associative*²⁸ model like (58), one can conversely explicitly construct the dissipation metric, which is rather the exceptional situation related to 1-dimensionality and uni-directionality of the considered delamination process.

6.2 Delamination in modes I, II and mixed modes

The dissipation in the so-called mode I (delamination by opening) is less than in the so-called mode II (delamination by shearing); sometimes, the difference may be tens or even hundreds of percents and, in general loading, it depends of the so-called *fracture-mode-mixity* angle, cf. [3, 50, 53, 92]. Microscopically, the additional dissipation in mode II may be explained by a certain plastic process both in the adhesive itself and in a narrow bulk vicinity of the delamination surface before the actual delamination starts, cf. [50, 99], or by some rough structure of the interface, cf. [31]. These plastic processes do not manifest in the mode I if the plastic strain is valued in $\mathbb{R}_{\text{dev}}^{d \times d}$ =the ‘incompressible’ (=trace free) symmetric strain, as usually considered. Modeling the narrow plastic stripe around Γ_C is computationally difficult, and thus the various simplified phenomenological models are worth considering.

An immediate reflection of the standard engineering approach as e.g. in [43, 93, 94] is to modify (45b) by an activation threshold $a = a(\psi)$ depending on the so-called *fracture-mode-mixity angle* ψ . For $\mathbb{K} = \text{diag}(\kappa_n, \kappa_t, \kappa_t)$, the latter is defined as

$$\psi = \psi(\llbracket u \rrbracket) := \arctan \sqrt{\frac{\kappa_t |\llbracket u \rrbracket_t|^2}{\kappa_n |\llbracket u \rrbracket_n|^2}} \quad (59)$$

where $\llbracket u \rrbracket_t$ and $\llbracket u \rrbracket_n$ stand for the tangential and the normal displacement jump, arising in the decomposition $\llbracket u \rrbracket = \llbracket u \rrbracket_n \nu + \llbracket u \rrbracket_t$ with $\llbracket u \rrbracket_n = \llbracket u \rrbracket \cdot \nu$ with ν a unit normal to Γ_C . Typical phenomenology is that $\kappa_t < \kappa_n$ (usually reaching no more than 80% of κ_n). A typical, phenomenological form of $a(\cdot)$ used in engineering [43] is, e.g.,

$$a(\psi) := a_I (1 + \tan^2((1-\lambda)\psi)) \quad (60)$$

where $a_I = a(0)$ is the activation threshold for fracture mode I and λ is the so-called *fracture-mode-sensitivity* parameter. E.g., for moderately strong fracture-mode sensitivity, which means the ratio a_{II}/a_I about 5-10 (with $a_{II} = a(90^\circ)$ being the activation threshold for the pure fracture mode II), one has λ about 0.2-0.3; cf. [94]. Therefore, this model uses the dissipation rate from Remark 3.8 in a general form, namely

$$\mathcal{R}(u, \dot{z}) := \begin{cases} \int_{\Gamma_C} a(\psi(\llbracket u \rrbracket)) |\dot{z}| \, dS & \text{if } \dot{z} \leq 0 \text{ on } \Gamma_C, \\ \infty & \text{otherwise.} \end{cases} \quad (61)$$

An immediate idea is to use a semi-implicit time discretization, leading to a modification of the incremental minimization problem (1) as follows

$$\left. \begin{array}{l} \text{minimize} \quad (u, z) \mapsto \mathcal{E}_{\mathbb{K}}(k\tau, u, z) + \mathcal{R}(u_\tau^{k-1}, z - z_\tau^{k-1}) \\ \text{subject to} \quad (u, z) \in \mathcal{U} \times \mathcal{Z}. \end{array} \right\} \quad (62)$$

²⁸Here “non-associative” means that there is no unique activation threshold associated to the dissipation mechanism. Sometimes, the meaning of the adjective “non-associative” rather means that the dissipative forces do not have any potential.

The convergence of this method is indeed guaranteed in some cases [61], in particular when the stored energy is uniformly convex. This, however, is not the case of $\mathcal{E}_{\mathbb{K}}$. The discrete stability inequality (18) is modified to

$$\mathcal{E}(k\tau, u_\tau^k, z_\tau^k) \leq \mathcal{E}(k\tau, \tilde{u}, \tilde{z}) + \mathcal{R}(u_\tau^{k-1}, \tilde{z} - z_\tau^k) \quad (63)$$

and the following energy inequalities hold:

$$\begin{aligned} & \mathcal{E}(k\tau, u_\tau^k, z_\tau^k) + \mathcal{R}(u_\tau^{k-1}, z_\tau^k - z_\tau^{k-1}) \\ & - \mathcal{E}((k-1)\tau, u_\tau^{k-1}, z_\tau^{k-1}) \leq \int_{(k-1)\tau}^{k\tau} \mathcal{E}'_t(t, u_\tau^{k-1}, z_\tau^{k-1}) dt \end{aligned} \quad (64)$$

and

$$\begin{aligned} & \mathcal{E}(k\tau, u_\tau^k, z_\tau^k) + \mathcal{R}(u_\tau^{k-2}, z_\tau^k - z_\tau^{k-1}) \\ & - \mathcal{E}((k-1)\tau, u_\tau^{k-1}, z_\tau^{k-1}) \geq \int_{(k-1)\tau}^{k\tau} \mathcal{E}'_t(t, u_\tau^k, z_\tau^k) dt . \end{aligned} \quad (65)$$

The first inequality follows from the minimality of (u_τ^k, z_τ^k) if compared with $(u_\tau^{k-1}, z_\tau^{k-1})$ while the second one is implied by the discrete stability (63) of $(u_\tau^{k-1}, z_\tau^{k-1})$ with $(\tilde{u}, \tilde{z}) = (u_\tau^k, z_\tau^k)$. We then get only $W^{1,1}$ bounds on piecewise affine interpolants of $\{z_\tau^k\}$. Hence, concentrations of \dot{z} can appear in the limit z which is thus a function of bounded variation, only. To pass to the limit in the dissipation term one would need to enhance sophisticated techniques developed in [2, 81] and only get the energy inequality. We refer to [37, 38] for more partial results. There is, however, an obvious peculiarity in direct application of the previous concepts from Remark 3.8 because the dissipation distance $\mathcal{D} = \mathcal{D}_{\mathcal{R}}$ defined implicitly by (32) here can be evaluated explicitly as $\mathcal{D}(q_1, q_2) = \int_{\Gamma_C} \min_{0 \leq \tilde{\psi} \leq \pi/2} a(\tilde{\psi}) |z_1 - z_2| dS$ if $z_2 \leq z_1$ a.e. on Γ_C , otherwise it is infinite. Existence of an energetic solution of such a model determined by $(\mathcal{E}_{\mathbb{K}}, \mathcal{D}_{\mathcal{R}})$ defined by (49) and (61) can be shown standardly, but such solutions do not distinguish particular modes at all. This is a quite-well known effect in non-associative models, indicating that sometimes other concepts of solutions are more relevant, cf. [60, 62]. Altogether, the analysis of (62) (or, e.g., a fully implicit modification of it) is not entirely clear. Moreover, a question remains, whether one can indeed model the desired mixity-sensitive effect in all situations in such a way. It is likely that higher gradients in u are needed to control $\llbracket u \rrbracket$ in $C(\bar{\Gamma}; \mathbb{R}^d)$ to give a good sense to $\int_0^T \mathcal{R}(u, \dot{z}) dt$ with $\mathcal{R}(u, \dot{z})$ from (61), i.e. to $\int_{\Gamma_C} a(\psi(\llbracket u \rrbracket)) |\dot{z}| dS$.

29

To overcome these drawbacks, but still considering an additional dissipation in mode II, one can alternatively consider an additional inelastic process on Γ_C . For this, we may introduce the dissipative variable s_p having the meaning of the “plastic” *tangential slip* s_p on Γ_C , and devise a plastic-like model with kinematic-type hardening for it, namely

$$\mathcal{Z} := L^\infty(\Gamma_C) \times L^2(\Gamma_C; \mathbb{R}^{d-1}), \quad \mathcal{X} := L^1(\Gamma_C) \times L^1(\Gamma_C; \mathbb{R}^{d-1}), \quad (66a)$$

²⁹In fact, this scenario indeed works in the viscous Kelvin-Voigt rheology from Section 6.5 below, as demonstrated recently in [84].

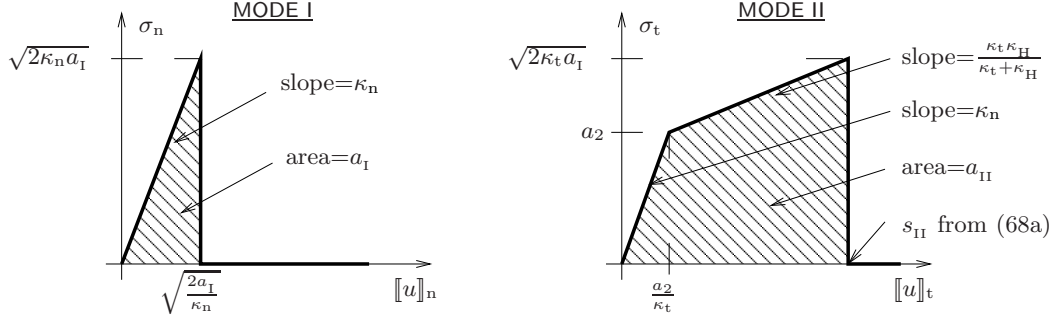


Figure 8: Schematic illustration of response of the mechanical stress in model (66) under pulling and shearing experiments; the left part (Mode I) corresponds to Fig. 6(right); $2\kappa_t a_I \geq a_2^2$ is supposed so that $a_{II} \geq a_I$.

$$\mathcal{E}(t, u, z, s_p) := \begin{cases} \sum_{i=1}^N \int_{\Omega_i} \mathbb{C}^{(i)} e(u) : e\left(\frac{u}{2} + u_D(t)\right) dx \\ + \int_{\Gamma_C} z \left(\frac{\kappa_n}{2} |[u]_n|^2 + \frac{\kappa_t}{2} |[u]_t - s_p|^2 \right) \\ + \frac{\kappa_H}{2} |s_p|^2 + \frac{\kappa_0}{r} |\nabla_s z|^r dS & \text{if } u = 0 \text{ on } \Gamma_D, \\ \infty & \text{if } [u]_n < 0 \text{ on } \Gamma_C, \\ & \text{if } 0 < z < 1 \text{ on } \Gamma_C, \\ & \text{elsewhere,} \end{cases} \quad (66b)$$

$$\mathcal{R}(\dot{z}, \dot{s}_p) := \begin{cases} \int_{\Gamma_C} a_I |\dot{z}| + a_2 |\dot{s}_p| dS & \text{if } \dot{z} \leq 0 \text{ a.e. on } \Gamma_C, \\ \infty & \text{otherwise,} \end{cases} \quad (66c)$$

with $[[u]] = [[u]]_n \nu + [[u]]_t$ with $[[u]]_n = [[u]] \cdot \nu$ with ν a unit normal to Γ_C , while \mathcal{U} is again from (43a). Rigorously, $s_p \in L^2(\Gamma_C; \mathbb{R}^{d-1})$ is considered as a $(d-1)$ -dimensional vector field embedded into \mathbb{R}^d space to give sense to the expression $[[u]]_t - s_p$. Like in (57), we use again a gradient theory for z with $r > d-1$ and $\kappa_0 > 0$ to facilitate the construction of the mutual recovery sequence.³⁰ In case $d = 3$, the physical dimensions are: $[a_I] = \text{J/m}^2$, $[a_2] = \text{J/m}^3$, and $[\kappa_t] = [\kappa_n] = [\kappa_H] = \text{J/m}^4$. The activation criterion to trigger the delamination is now

$$\frac{1}{2} \left(\kappa_n |[u]_n|^2 + \kappa_t |[u]_t - s_p|^2 \right) \leq a_I. \quad (67)$$

Starting from the initial conditions $s_{p,0} = 0$ and $z_0 = 1$, the response in the pure Mode I is essentially the same as on Fig. 6(right), because no evolution of s_p is triggered by mere opening. To analyze the response in the pure Mode II, let us realize that the tangential stress σ_t is a derivative of \mathcal{E} with respect to $[[u]]_t$, and thus $\sigma_t(u, s_p) = \kappa_t ([[u]]_t - s_p)$ if $z = 1$. In analogy to the plasticity, the slope of evolution of s_p under hardening is $\kappa_t / (\kappa_t + \kappa_H)$. From (67), one can see that the delamination is triggered if $\frac{1}{2} \kappa_t |[u]_t - s_p|^2 = \frac{1}{2} \sigma_t^2 / \kappa_t$ reaches the threshold a_I , i.e. if the tangential stress σ_t achieves the threshold $\sqrt{2a_I \kappa_t}$, as depicted on Fig. 8(right). The delamination in Mode II is thus triggered under the tangential displacement

$$s_{II} = \frac{\sqrt{2\kappa_t^3 a_I} - a_2 \kappa_t + \sqrt{2\kappa_t \kappa_H^2 a_I}}{\kappa_t \kappa_H} \quad (68a)$$

³⁰We can use the damage-type construction for z , i.e., $\tilde{z}_k = (\tilde{z} - \|z - z_k\|_{L^\infty(\Gamma_C)})^+$ and the binomial trick [65] for s_p ; cf. [83] for details.

and, after some algebra, one can see that the overall dissipated energy is

$$a_{\text{II}} = a_{\text{I}} + \frac{a_2}{\kappa_{\text{H}}} \left(\sqrt{2\kappa_{\text{t}} a_{\text{I}}} - a_2 \right) \quad (68b)$$

provided $2\kappa_{\text{t}} a_{\text{I}} \geq a_2^2$. The *fracture-mode sensitivity* $a_{\text{II}}/a_{\text{I}}$ is then indeed bigger than 1, namely $1 + a_2(\sqrt{2\kappa_{\text{t}} a_{\text{I}}} - a_2)/(\kappa_{\text{H}} a_{\text{I}})$. The surface plastic slip stops evolving after delamination and as used for (68b) only if, after the delamination, the driving stress $\kappa_{\text{H}} s_{\text{II}}$ has the magnitude less than a_2 . In view of (68a), it needs $\kappa_{\text{t}} a_{\text{I}} < 2a_2^2$. Thus, to produce desired effects, our model should work with parameters satisfying

$$\frac{1}{2} \kappa_{\text{t}} a_{\text{I}} < a_2^2 \leq 2\kappa_{\text{t}} a_{\text{I}}. \quad (69)$$

The validity of this model has been tested numerically in [54, 83].

An interesting open problem is the limit passage of this model under a suitable scaling to a brittle model like in Proposition 5.1.

Let us note that, in both of the mixity-sensitive models considered in this section, the stored energy involves z linearly. Yet, it is not difficult to combine *cohesive-zone-type models* from Section 6.1 with these mixity-sensitive models. Thus, e.g., (61) can be generalized to

$$\mathcal{R}(u, z, \dot{z}) := \begin{cases} \int_{\Gamma_{\text{C}}} a(\psi(\llbracket u \rrbracket), z) |\dot{z}| \, dS & \text{if } \dot{z} \leq 0 \text{ on } \Gamma_{\text{C}}, \\ \infty & \text{otherwise.} \end{cases} \quad (70)$$

To facilitate the mathematical analysis, one again needs the stored energy to be augmented by the delamination gradient.

The influence of the mixed-mode behavior will be illustrated on an example of the mixed-mode flexure test [101, Section 3.2] shown in Figure 9. The material properties of the bulk material are the same as in Section 5.3, the elastic-brittle interface is now characterized by the stiffnesses $\kappa_{\text{n}} = 810 \text{ GPa/m}$, $\kappa_{\text{t}} = 760 \text{ GPa/m}$. The mode-I and mode-II fracture energies are set to values $a_{\text{I}} = 200 \text{ Jm}^{-2}$ and $a_{\text{II}} = 900 \text{ Jm}^{-2}$, in order to achieve a more ductile structural response. The prescribed mid-span displacement equals to 2.5 mm at $T = 1$. The non-associative model (61) with (49) is used.

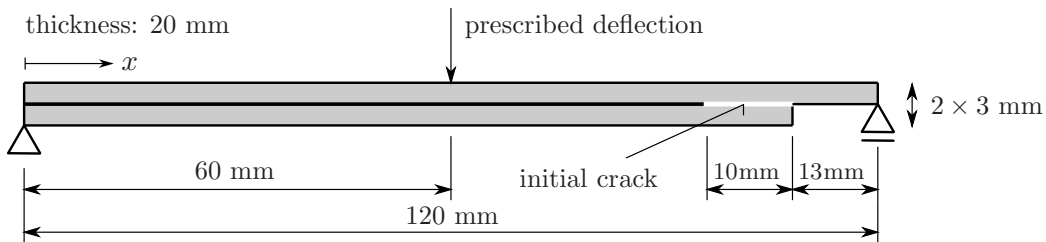


Figure 9: Setup of the mixed-mode flexure test.

Figure 10(a) summarizes the energetics of the delamination evolution. After the initial elastic regime, the delamination initiates in a combined normal and shear modes, cf. Figure 10(b). This accompanied by high a increase of the dissipated energy. With the increasing load, however, the mode mixity gradually changes towards the opening mode. The production of the dissipated energy decreases and the interfacial stored energy almost vanishes; see also Figure 11 for an illustration. The response remains almost independent of the mesh size h . Moreover, the back-tracking algorithm remained inactive for the whole loading range, which confirms the energy stability of the delamination evolution. Note that the peaks in the mode-mixity angles in Figure 10(b) are related to changes of the sign of the tangential slip $\llbracket u \rrbracket_{\text{t}}$, recall Eq. (59).

Remark 6.1 (Mode III) Delamination by twisting (i.e. Mode III) exhibits specific behavior and is often considered in addition, but we did not focus on this sort of models here. In fact, it would be possible to model such regimes by making the activation threshold dependent on the angle between $\nabla_s z$ and the tangential stress. Obviously, it needs compactness in terms of $\nabla_s z$ which would have to occur “nonlinearly” in the model, so that an even higher gradient of z should be involved in \mathcal{E} .

6.3 Multi-threshold delamination

Some engineering literature incorporates the concept of parallel breakable springs with different elastic and inelastic properties, cf. [94, 93]. On the continuum-mechanical level, this idea can be reflected by a generalization of the previous model by considering J different adhesives acting simultaneously on Γ_C :

$$\mathcal{E}(t, u, z_1, \dots, z_J) := \begin{cases} \sum_{i=1}^N \int_{\Omega_i} \mathbb{C}^{(i)} e(u) : e\left(\frac{u}{2} + u_D(t)\right) dx \\ + \int_{\Gamma_C} \frac{\sum_{j=1}^J z_j \mathbb{K}_j \llbracket u \rrbracket}{2} \cdot \llbracket u \rrbracket dS \\ \infty \end{cases} \quad \begin{cases} \text{if } u = 0 \text{ on } \Gamma_D, \\ \llbracket u \rrbracket_n \geq 0 \text{ on } \Gamma_C \\ 0 \leq z_j \leq 1 \text{ on } \Gamma_C, \\ \text{elsewhere,} \end{cases} \quad (71a)$$

$$\mathcal{R}(\dot{z}_1, \dots, \dot{z}_J) := \begin{cases} \sum_{j=1}^J \int_{\Gamma_C} a_j |\dot{z}_j| dS & \text{if } \max_{j=1, \dots, J} \dot{z}_j \leq 0 \text{ on } \Gamma_C, \\ \infty & \text{otherwise.} \end{cases} \quad (71b)$$

Again, the advantage of the energetic formulation is that there is no problem to combine the multi-threshold models with the cohesive-zone models from Section 6.1 and/or the mixity-sensitive models from Section 6.2. Also, instead of parameterizing the various adhesives by a discrete parameter $j = 1, \dots, J$, one could use a “continuous” parameter.

6.4 Combination with other inelastic processes

The definite advantage of the energetic formulation is that one can easily combine the above presented delamination models with other inelastic processes, like damage or plasticity in the bulk.

Let us illustrate it by a simple example, augmenting the model from Sect. 5 by linearized, single-threshold *plasticity* with kinematic *hardening*. The additional variable is then the plastic strain π valued in $\mathbb{R}_{\text{dev}}^{d \times d} := \{\pi \in \mathbb{R}^{d \times d}, \pi^\top = \pi, \text{tr } \pi = 0\}$, and the plastic response is determined by the convex “elasticity” domain $S^{(i)} \subset \mathbb{R}_{\text{dev}}^{d \times d}$ and by a hardening tensor $\mathbb{H}^{(i)}$ on each Ω_i . After making the shift of the Dirichlet conditions, the functionals read:

$$\mathcal{E}_{\mathbb{K}}(t, u, z, \pi) := \begin{cases} \sum_{i=1}^N \int_{\Omega_i} \mathbb{C}^{(i)} (e(u) - \pi) : \left(e\left(\frac{u}{2} + u_D(t)\right) - \frac{\pi}{2} \right) + \mathbb{H}^{(i)} \pi : \pi dx \\ + \int_{\Gamma_C} \frac{1}{2} z \mathbb{K} \llbracket u \rrbracket \cdot \llbracket u \rrbracket dS \\ \infty \end{cases} \quad \begin{cases} \text{if } u = 0 \text{ on } \Gamma_D, \\ \llbracket u \rrbracket_n \geq 0 \text{ on } \Gamma_C, \\ 0 \leq z \text{ on } \Gamma_C, \\ \text{elsewhere,} \end{cases} \quad (72a)$$

$$\mathcal{R}(\dot{z}, \dot{\pi}) := \begin{cases} \int_{\Gamma_C} a|\dot{z}| \, dS + \sum_{i=1}^N \int_{\Omega_i} \delta_{S^{(i)}}^*(\dot{\pi}) \, dx & \text{if } \dot{z} \leq 0 \text{ on } \Gamma_C, \\ \infty & \text{otherwise.} \end{cases} \quad (72b)$$

and, instead of (43b),

$$\mathcal{L} := L^\infty(\Gamma_C) \times L^2(\Omega; \mathbb{R}_{\text{dev}}^{d \times d}). \quad (72c)$$

The classical formulation corresponding to (6) with \mathcal{E} and \mathcal{R} from (45b) consists in equilibrium of forces on each subdomain Ω_i and four complementarity problems on Γ_C , corresponding to the four subdifferentials occurring in the involved functionals $\mathcal{E}_{\mathbb{K}}$ and \mathcal{R} . Before making the shift of the Dirichlet conditions, it reads as:

$$\left. \begin{aligned} \operatorname{div} \sigma &= 0, & \sigma &= \mathbb{C}^{(i)}(e(u) - \pi), \\ \dot{\pi} &\in N_{S^{(i)}}(\mathbb{H}^{(i)}\pi - \sigma), \end{aligned} \right\} \quad \text{in } \Omega_i, \quad i = 1, \dots, N, \quad (73a)$$

$$u = w_D(t, \cdot) \quad \text{on } \Gamma_D, \quad (73b)$$

$$\sigma \nu = 0 \quad \text{on } \Gamma_N, \quad (73c)$$

$$\left. \begin{aligned} \llbracket \sigma \rrbracket \nu &= 0 \\ \sigma \nu + z \mathbb{K} \llbracket u \rrbracket &= 0 \\ \llbracket u \rrbracket_n \geq 0, \quad \sigma_n(u) \leq 0, \quad \sigma_n(u) \llbracket u \rrbracket_n &= 0 \\ \dot{z} \leq 0, \quad \frac{1}{2} \mathbb{K} \llbracket u \rrbracket \cdot \llbracket u \rrbracket + \rho &\leq a \\ \dot{z} \left(\frac{1}{2} \mathbb{K} \llbracket u \rrbracket \cdot \llbracket u \rrbracket + \rho - a \right) &= 0 \\ z \geq 0, \quad \rho \leq 0, \quad \rho z &= 0, \end{aligned} \right\} \quad \text{on } \Gamma_C, \quad (73d)$$

where $N_{S^{(i)}}$ denotes the normal cone to $S^{(i)}$, similarly like in (10).

There are both mathematical and engineering studies combining elasto-plasticity with cracks, cf. e.g. [7, 24]; this is a highly nontrivial problem because the crack path is not a-priori prescribed, in contrast to delamination and, besides, the perfect (so-called Prandtl-Reuss) plasticity has been considered in [24]. Combination with damage models in the bulk is also easily possible. Even, recent studies [66, 95] reveal that the delamination model from Sect. 4 can be obtained as the limit when, instead of a surface Γ_C undergoing delamination, one considers a narrow stripe of material undergoing damage and passes the thickness of that stripe to zero. A challenging conjecture is whether also the refined models from Sect. 6 can be justified in such a way, e.g. considering a narrow stripe of a material undergoing damage and plasticity with kinematic hardening might recover the mixity-dependent model (66) under a suitable scaling. This could support former engineering studies as e.g. in [99, 102].

6.5 Dynamical adhesive contact in visco-elastic materials

So far, we considered only quasi-static models, which have relatively broad applicability. In some situations, more effects must be taken into account, however. In particular, even under very slow loading, spontaneous rupture of weak surfaces Γ_C may lead to the emission of elastic waves in the bulk, that may backward interact with the rate-independent delamination hosted on Γ_C . Thus inertial effects are to be considered. It is natural to take into account also an attenuation in the bulk. Considering the Kelvin-Voigt rheology, the simplest model from Sect. 5 thus modifies as:

$$\varrho^{(i)} \ddot{u} - \operatorname{div} \sigma = 0, \quad \sigma = \mathbb{C}^{(i)} e(u) + \mathbb{D}^{(i)} e(\dot{u}) \quad \text{in } \Omega_i, \quad i = 1, \dots, N, \quad (74a)$$

$$u = w_D(t, \cdot) \quad \text{on } \Gamma_D, \quad (74b)$$

$$\sigma \nu = 0 \quad \text{on } \Gamma_N, \quad (74c)$$

$$\left. \begin{aligned} & \llbracket \sigma \rrbracket \nu = 0 \\ & \sigma \nu + z \mathbb{K} \llbracket u \rrbracket = 0 \\ & \llbracket u \rrbracket_n \geq 0, \quad \sigma_n(u) \leq 0, \quad \sigma_n(u) \llbracket u \rrbracket_n = 0, \\ & \dot{z} \leq 0, \quad \frac{1}{2} \mathbb{K} \llbracket u \rrbracket \cdot \llbracket u \rrbracket + \rho \leq a \\ & \dot{z} \left(\frac{1}{2} \mathbb{K} \llbracket u \rrbracket \cdot \llbracket u \rrbracket + \rho - a \right) = 0 \\ & z \geq 0, \quad \rho \leq 0, \quad \rho z = 0. \end{aligned} \right\} \quad \text{on } \Gamma_C, \quad (74d)$$

where $\varrho^{(i)} > 0$ is a mass density and $\mathbb{D}^{(i)}$ is a 4th-order symmetric positive definite tensor determining the attenuation of the material occupying the domain Ω_i . This model is analyzed by a semidiscretization in time leading to a recursive increment formula. We refer to [82] for more details.

For an analogous model but with viscous (instead of the activated rate-independent) adhesion we refer to [90, Chap.5] or e.g. [22] and, with plasticity in the bulk, to [44].

The typical application of dynamic adhesive contact is in the modeling of spontaneous rupture on lithospheric faults (=weak surfaces in the language of mechanical engineers) with the emission of elastic waves having the capability to trigger e.g. another possible rupture on an adjacent fault and inelastic damage in particular on the Earth surface as *earthquakes*. Typical rupture processes run in pure Mode II because the enormous gravity pressures on the faults deep under the Earth surface exclude Mode I. Thus, also the Signorini contact might be even a-priori simplified to the condition $\llbracket u \rrbracket_n = 0$ on Γ_C . An important phenomenon to facilitate spontaneous rupture within earthquake modeling is the so-called *slip weakening*; cf. models and discussion e.g. in [1, 9, 18, 26, 48, 52, 100]. There are several options how to describe the weakening phenomena within the models presented above. One can, e.g., modify model (66) by considering the activation threshold a_1 in (66c) dependent on the plastic slip s_p or, perhaps more physically, on $\int_0^t |\dot{s}_p| dt$, which then turns the dissipation to be non-associative.

Another possibility arises if $\mathcal{E}(t, u, \cdot)$ is concave. In model (57) in Sect. 6.1 with $\mathbb{K}_1 = \kappa_1 \mathbb{I}$ and $\mathbb{K}_2 = \kappa_2 \mathbb{I}$, this occurs if κ_2 is small, namely $0 > \kappa_2 > -\kappa_1/2$. Then Figure 6 is relevant but the rupture happens under the mechanical stress $\sigma = (\kappa_1 + \kappa_2) \sqrt{2a/(\kappa_1 + 2\kappa_2)}$ when $\llbracket u \rrbracket = \sqrt{2a/(\kappa_1 + 2\kappa_2)}$ like in Figure 7. Thus, one can model *delamination weakening*. Note that the initial stress σ leading to delamination may be made very large by sending $\kappa_2 \downarrow -\kappa_1/2$, even if the total dissipated energy may be independently moderate. One can see the weakening effect also from (58): if $\kappa_2 < 0$, then ϕ is strictly concave, hence ϕ' is decreasing, and thus the effective activation threshold (58) gets smaller if η decreases (ranging over a monotone branch of ϕ , of course).

The weakening phenomenon may also occur in the multi-threshold models from Sect. 6.3: considering $\mathbb{K}_1 > \mathbb{K}_2 > \dots$ (=ordering of positive definite matrices) and $a_1 > a_2 > \dots$, initially the first adhesive bears high stress but, when debonded, the next adhesives can bear less and less stress.

6.6 Thermodynamics of adhesive contact

Interesting features might be triggered in non-isothermal situations. Mechanical stresses in thermally expanding materials can be created by spatially varying temperature profiles. Also, merging materials with different thermal expansion (as typical in laminated composites) creates mechanical stresses even for spatially equilibrated temperature. Such a thermo-mechanical load may lead to delamination. This may naturally influence the heat transfer through delaminated surfaces. Hence, besides the usual thermo-mechanical cou-

pling due to viscous dissipation and thermal expansion in the bulk, also another coupling by delamination is occurring.

Focusing again on Kelvin-Voigt rheology as in Sect. 6.5, the thermodynamically consistent model, naturally involving the additional variable θ as temperature, reads as

$$\left. \begin{aligned} \rho \ddot{u} - \operatorname{div} \sigma &= 0, \\ \sigma &= \mathbb{C}^{(i)}(e(u) - \theta \mathbb{E}^{(i)}) + \mathbb{D}^{(i)}e(\dot{u}), \\ c^{(i)}(\theta) \dot{\theta} - \operatorname{div}(\mathbb{L}^{(i)} \nabla \theta) &= (\mathbb{D}^{(i)}e(\dot{u}) - \theta \mathbb{C}^{(i)} \mathbb{E}^{(i)}) : e(\dot{u}) \end{aligned} \right\} \quad \text{in } \Omega_i, \quad (75a)$$

$$u = w_D(t, \cdot) \quad \text{on } \Gamma_D, \quad (75b)$$

$$\sigma \nu = 0 \quad \text{on } \Gamma_N, \quad (75c)$$

$$\left. \begin{aligned} \llbracket \sigma \rrbracket \nu &= 0 \\ \sigma \nu + z \mathbb{K} \llbracket u \rrbracket &= 0 \\ \llbracket u \rrbracket_n &\geq 0, \quad \sigma_n(u) \leq 0, \quad \sigma_n(u) \llbracket u \rrbracket_n = 0, \\ \dot{z} &\leq 0, \quad \frac{1}{2} \mathbb{K} \llbracket u \rrbracket \cdot \llbracket u \rrbracket + \rho \leq a = a_0 + a_1 \\ \dot{z} \left(\frac{1}{2} \mathbb{K} \llbracket u \rrbracket \cdot \llbracket u \rrbracket + \rho - a \right) &= 0 \\ z &\geq 0, \quad \rho \leq 0, \quad \rho z = 0. \\ \llbracket \mathbb{L} \nabla \theta \rrbracket \cdot \nu &= -a_1 \dot{z}, \\ \ll \mathbb{L} \nabla \theta \cdot \nu \gg + \eta(\llbracket u \rrbracket, z) \llbracket \theta \rrbracket &= 0 \end{aligned} \right\} \quad \text{on } \Gamma_C, \quad (75d)$$

where $\ll \cdot \gg$ denotes the average of traces from both sides of Γ_C , and where $\mathbb{E}^{(i)}$ is the matrix of thermal-expansion coefficients which may depend on Ω_i similarly as $\mathbb{C}^{(i)}$ and $\mathbb{D}^{(i)}$, further $c^{(i)} = c^{(i)}(\theta)$ is the heat capacity, and $\mathbb{L}^{(i)}$ is the positive-definite heat-conductivity tensor, and $\eta = \eta(\llbracket u \rrbracket, z)$ is the heat-transfer coefficient through the delaminating boundary Γ_C .

Note that only a part $a_1/a = a_1/(a_1+a_0)$ of the mechanical energy dissipated during delamination contributes to the heat production on Γ_C , while the rest a_0/a is irreversibly stored (=dissipated) in the debonded adhesive without contributing to the heat balance.

Mode II heats up considerably more than Mode I, as experimentally documented in [80]. E.g., having in mind (76), one may consider the splitting

$$a_0(\psi) := a_1, \quad a_1(\psi) := a_1 \tan^2((1-\lambda)\psi), \quad (76)$$

meaning that the plain delamination does not contribute to the heat production at all, and only the additional dissipation related with Mode II contributes to the heat production on the delaminating surface.

For model (66), it would be natural to involve the dissipation via $a_2 |\dot{s}_d|$ as a measure-valued heat source acting on Γ_C while the dissipation by pure opening along the surface, i.e. $a_1 |\dot{z}|$, would contribute rather to the stored energy. Mathematical analysis of such a problem, as well as numerical experiments, seem challenging. For the mixity-independent dissipation, this model has been analyzed in [85] while the Griffith-type rate-dependent adhesion see also [14]. Recently, also mixity-sensitive dissipation was scrutinized in [84] by implementing the concept of hyperstresses.

7 Conclusion and further application

We surveyed some known models and proposed a menagerie of new ones for delamination under small strains. The main purpose has been to cover them in a unified concept of quasistatic evolution of the form (6) or (30), also pursuing their energetics, and outline their rigorous mathematical and numerical analysis based on the concept of the so-called energetic solutions. This suggests efficient computational algorithms and allows for mathematically supported simulations. It also allows relatively easily and routinely to combine various mutually competing inelastic processes both on the delaminating surface or in

the bulk, and to devise advanced mathematically supported models and launch numerical simulations of such nontrivial processes. In addition, under certain conditions, it may also be combined with some rate-dependent processes in the bulk, such as viscosity in a sufficiently dissipating rheology (as Kelvin-Voigt's one), inertia, and even thermal processes as, e.g., thermo-visco-plasticity.

Although the focus of this chapter was on the modeling of macroscopic delamination problems, the presented framework can easily be adapted also to the homogenization of composites with debonding interfaces. In the context of two-scale homogenization, the stored energy associated to the unit cell problem reads [57, 71]:

$$\mathcal{E}_{\mathbb{K}}(t, u, z) := \begin{cases} \sum_{i=1}^N \frac{1}{2} \int_{\Omega_i} \mathbb{C}^{(i)}(e(u)+E(t)) : (e(u)+E(t)) \, dx \\ + \int_{\Gamma_C} \frac{1}{2} \phi(z) \mathbb{K} \llbracket u \rrbracket \cdot \llbracket u \rrbracket + \frac{\kappa_0}{r} |\nabla_S z|^r \, dS & \text{if } u \text{ is } \Omega\text{-periodic,} \\ \int_{\Omega} u \, dx = 0, \\ \llbracket u \rrbracket_n \geq 0 \text{ on } \Gamma_C, \\ 0 \leq z \text{ on } \Gamma_C, \\ \infty & \text{elsewhere,} \end{cases}$$

where $E(t)$ designates the macroscopic strain tensor, u now denotes a periodic microscopic displacement and the function ϕ is used to model the cohesive contact with a piecewise linear traction-separation law, recall Section 6. The dissipative potential remains unchanged, as well as the numerical treatment of the incremental problem. The periodic boundary conditions and the macroscopic strain are incorporated by the Lagrange multipliers technique introduced, e.g., in [56]. As an example, we consider a cross-section of a unit cell of a fiber-reinforced composite, subject to a bi-axial macroscopic stretching $E_{11} = E_{22} = 1.5\%$ at $T = 1$. Geometry of the problem is defined by the fiber volume fraction equal to 50% and the diameter of the fiber taken as 10 μm . The material data of individual phases and interfaces appear in Table 7; the gradient term was neglected by putting $\kappa_0 = 0$.

Material data

Matrix Young's modulus	1 MPa
Matrix Poisson's ratio	0.4
Fiber Young's modulus	150 MPa
Fiber Poisson's ratio	0.3
Interfacial fracture energy, a	0.02 J/m ²
Interfacial elastic stiffnesses, $\kappa_n = \kappa_t$	0.5 GPa/m
Interfacial cohesive contact function	$\phi(z) = z/(1-z+10^{-4})$

The energetics of the progressive debonding is in Figure 12, together with representative snapshots of debonding evolution. Due to the prescribed cohesive law, we capture the gradual transition from a stiff elastic interface, i.e., when the highest values of stresses are found in the fiber, to the completely debonded configuration. In this situation all load is carried by the matrix phase and the stored interfacial energy drops to zero.

This simple study is complemented with a numerical simulation of debonding evolution in a complex 20-particle unit cell subject to macroscopic shear $E_{12} = 1\%$. The results appearing in Figure 13 confirm that the energetic approach, combined with robust duality-based solvers, allows for capturing complex mechanisms of multiple contact, sliding and gradual damage between fibers and matrix in geometrically complicated real-world material samples.

We entirely omitted models at large strains. Let us, however, point out that the advantage of the energetic formulation is that the quasistatic delamination models can be relatively easily formulated also in large strains, in contrast to dynamical viscous models of the type (74).

Acknowledgments The authors warmly thank Vladislav Mantič, Ctirad Matyska, Alexander Mielke, Riccarda Rossi and Marita Thomas for many fruitful discussions and comments, and Pavel Gruber for performing numerical simulations. We extend our thanks to two anonymous referees whose valuable remarks and suggestions helped us to improve the clarity of the original manuscript. The authors also acknowledge partial support from the grants A 100750802 (GA AV ČR), 106/08/1379, 201/09/0917, 106/09/1573, and 201/10/0357 (GA ČR), MSM 21620839 and VZ6840770021 (MŠMT ČR), and from the research plan AV0Z20760514 (ČR). T.R. also acknowledges the hospitality of Universidad de Sevilla, where this work has partly been accomplished, covered by Junta de Andalucía through the project IAC 09-III-6321.

References

- [1] R.E. Abercrombie and J.R. Rice. Can observations of earthquake scaling constrain slip weakening. *Geophys. J. Int.*, 162:406–424, 2005.
- [2] E. Balder. A general approach to lower semicontinuity and lower closure in optimal control theory. *SIAM J. Control. Optim.*, 22:570–598, 1984.
- [3] L. Banks-Sills and D. Askenazi. A note on fracture criteria for interface fracture. *Intl. J. Fracture*, 103:177–188, 2000.
- [4] S. Bartels and T. Roubíček. Thermo-visco-elasticity with rate-independent plasticity in isotropic materials undergoing thermal expansion. *Math. Model. Numer. Anal.*, 45:477–504, 2011.
- [5] B. Benešová. Modeling of shape-memory alloys on the mesoscopic level. In P. Šittner et al., editor, *Proc. ESOMAT 2009*, pages 1–7. EDP Sciences, 2009.
- [6] B. Benešová. Global optimization numerical strategies for rate-independent processes. (Preprint no. 2010-002, Nečas center, Charles Univ., Prague, 2010). *J. Global Optim. (in print)*, 2011.
- [7] D. Bigoni and E. Radi. Mode I crack propagation in elastic-plastic pressure-sensitive materials. *Intl. J. Solids Struct.*, 30:899–919, 1993.
- [8] M.A. Biot. *Mechanics of Incremental Deformations*. Wiley, New York, 1965.
- [9] A. Bizzarri and M. Cocco. 3D dynamic simulations of spontaneous rupture propagation governed by different constitutive laws with rake rotation allowed. *Ann. Geophys.*, 48:279–299, 2005.
- [10] A. Blázquez, V. Mantič, and F. París. Application of BEM to generalized plane problems for anisotropic elastic materials in presence of contact. *Eng. Anal. Bound. Elem.*, 30:489–502, 2006.
- [11] A. Blázquez, R. Vodička, F. París, and V. Mantič. Comparing the conventional displacement BIE and the BIE formulations of the first and second kind in frictionless contact problems. *Eng. Anal. Bound. Elem.*, 26:815–826, 2002.
- [12] E. Bonetti, G. Bonfanti, and R. Rossi. Well-posedness and long-time behaviour for a model of contact with adhesion. *Indiana Univ. Math. J.*, 56:2787–2820, 2007.
- [13] E. Bonetti, G. Bonfanti, and R. Rossi. Global existence for a contact problem with adhesion. *Math. Meth. Appl. Sci.*, 31:1029–1064, 2008.
- [14] E. Bonetti, G. Bonfanti, and R. Rossi. Thermal effects in adhesive contact: modelling and analysis. *Nonlinearity*, 22:2697–2731, 2009.
- [15] J. Bouchala, Z. Dostál, and M. Sadowská. Scalable total BETI based algorithm for 3D coercive contact problems of linear elastostatics. *Computing*, 85, 2009.
- [16] B. Bourdin. Numerical implementation of the variational formulation for quasi-static brittle fracture. *Interfaces and Free Boundaries*, 9:411–430, 2007.
- [17] B. Bourdin, G. A. Francfort, and J.-J. Marigo. Numerical experiments in revisited brittle fracture. *J. Mech. Phys. Solids*, 48:797–826, 2000.
- [18] J. Burjánek. *Dynamic stress field of kinematic earthquake source models*. PhD thesis, Math.-Phys. Faculty, Charles Univ., 2006.
- [19] S. Burke, C. Ortner, and E. Süli. An adaptive finite element approximation of a variational model of brittle fracture. *SIAM J. Numer. Anal.*, 48:980–1012, 2010.

- [20] F. Cagnetti. A vanishing viscosity approach to fracture growth in a cohesive zone model with prescribed crack path. *Math. Models Meth. Appl. Sci.*, 18:1027–1071, 2009.
- [21] C. Carstensen, K. Hackl, and A. Mielke. Non-convex potentials and microstructures in finite-strain plasticity. *Proc. Royal Soc. London Ser. A*, 458:299–317, 2002.
- [22] M. Cocou, M. Schryve, and M. Raous. A dynamic unilateral contact problem with adhesion and friction in viscoelasticity. *Zeitschrift Angew. Math. Phys.*, 61:721743, 2010.
- [23] B. Dacorogna. *Direct Methods in the Calculus of Variations*, 2nd ed. Springer, New York, 2008.
- [24] G. Dal Maso and R. Toader. Quasistatic crack growth in elasto-plastic materials: the two-dimensional case. *Arch. Rational Mech. Anal.*, 196:867–906, 2010.
- [25] G. Dal Maso and C. Zanini. Quasi-static crack growth for a cohesive zone model with prescribed crack path. *Proc. R. Soc. Edinb., Sect. A, Math.*, 137(2):253–279, 2007.
- [26] S. Das. Spontaneous complex earthquake rupture propagation. *Pure Appl. Geophysics*, 160:579–602, 2003.
- [27] G. Del Piero and M. Raous. A unified model for adhesive interfaces with damage, viscosity, and friction. *European J. Mech. - A/Solids*, 29:496–507, 2010.
- [28] Z. Dostál. *Optimal Quadratic Programming Algorithms: With Applications to Variational Inequalities*. Springer, New York, 2009.
- [29] Z. Dostál, T. Kozubek, V. Vondrák, T. Brzobohatý, and A. Markopoulos. Scalable TFETI algorithm for the solution of multibody contact problems of elasticity. *Int. J. Numer. Meth. Engng.*, 82:1384–1405, 2010.
- [30] I. Ekeland and R. Temam. *Convex Analysis and Variational Problems*. SIAM, Philadelphia, 1999.
- [31] A.G. Evans, M. Rühle, B.J. Dalgleish, and P.G. Charalambides. The fracture energy of bimaterial interfaces. *Metall. Mater. Trans. A-Phys. Metall. Mater. Sci.*, 21A:2419–2429, 1990.
- [32] G. Francfort and A. Mielke. Existence results for a class of rate-independent material models with nonconvex elastic energies. *J. reine angew. Math.*, 595:55–91, 2006.
- [33] M. Frémond. *Non-Smooth Thermomechanics*. Springer, Berlin, 2002.
- [34] E. Graciani, V. Mantič, F. París, and A. Blázquez. Weak formulation of axi-symmetric frictionless contact problems with boundary elements. Application to interface crack. *Comput. Struct.*, 83:836–855, 2005.
- [35] E. Graciani, V. Mantič, F. París, and J. Varna. Numerical analysis of debond propagation in the single fibre fragmentation test. *Composites Science and Technology*, 69:2514–2520, 2009.
- [36] A.A. Griffith. The phenomena of rupture and flow in solids. *Philos. Trans. Royal Soc. London Ser. A. Math. Phys. Eng. Sci.*, 221:163–198, 1921.
- [37] P. Gruber, M. Kružík, and J. Zeman. Numerical approach to decohesion models with state-dependent dissipation. *in preparation*.
- [38] P. Gruber, J. Zeman, and J. Kruis. Numerical modeling of delamination via incremental energy minimization and duality-based solvers. *in preparation*.
- [39] K. Hackl and F. D. Fischer. On the relation between the principle of maximum dissipation and inelastic evolution given by dissipation potential. *Proc. Royal Soc. A*, 464:117–132, 2007.
- [40] B. Halphen and Q.S. Nguyen. Sur les matériaux standards généralisés. *J. Mécanique*, 14:39–63, 1975.
- [41] W. Han and B.D. Reddy. *Plasticity (Mathematical Theory and Numerical Analysis)*, volume 9 of *Interdisciplinary Applied Mathematics*. Springer-Verlag, New York, 1999.
- [42] R. Hill. A variational principle of maximum plastic work in classical plasticity. *Q.J. Mech. Appl. Math.*, 1:18–28, 1948.
- [43] J.W. Hutchinson and T.Y. Wu. Mixed mode cracking in layered materials. In T.Y. Wu J.W. Hutchinson, editor, *Advances in Applied Mechanics*, pages 63–191. Acad. Press, New York, 1992.
- [44] J. Jarušek and M. Sofonea. On the solvability of dynamic elastic-visco-plastic contact problems with adhesion. *Annals Acad. Romanian Sci.*, 1:191–214, 2009.

- [45] D. Knees, A. Mielke, and C. Zanini. On the inviscid limit of a model for crack propagation. *Math. Models Meth. Appl. Sci. (M³AS)*, 18:1529–1569, 2008.
- [46] D. Knees and A. Schröder. Numerical convergence analysis for a vanishing viscosity fracture model. In preparation.
- [47] D. Knees, C. Zanini, and A. Mielke. Crack growth in polyconvex materials. *Physica D*, 239:1470–1484, 2010.
- [48] B.V. Kostrov and S. Das. *Principles of Earthquake Source Mechanics*. Cambridge Univ. Press, New York, 1988.
- [49] M. Kočvara, A. Mielke, and T. Roubíček. A rate-independent approach to the delamination problem. *Math. Mechanics Solids*, 11:423–447, 2006.
- [50] K.M. Liechti and Y.S. Chai. Asymmetric shielding in interfacial fracture under in-plane shear. *J. Appl. Mech.*, 59:295–304, 1992.
- [51] J. Lubliner. A maximum dissipation principle in generalized plasticity. *Acta Mech.*, 52:225–237, 1984.
- [52] R. Madariaga and K.B. Olsen. Earthquake dynamics. In W. Lee et al., editor, *Intl. Handbook of Earthquake and Engineering Seismology*. Acad. Press, London, 2002.
- [53] V. Mantič. Discussion on the reference length and mode mixity for a bimaterial interface. *J. Engr. Mater. Technology*, 130:045501–1–2, 2008.
- [54] V. Mantič, C.G. Panagiotopoulos, and T. Roubíček. Associative quasistatic mixed-mode delamination model and its BEM implementation. in preparation.
- [55] G.A. Maugin. *The Thermomechanics of Plasticity and Fracture*. Cambridge University Press, Cambridge, 1992.
- [56] J.C. Michel, H. Moulinec, and P. Suquet. Effective properties of composite materials with periodic microstructure: a computational approach. *Comput. Methods Appl. Mech. Engrg.*, 172:109–143, 1999.
- [57] C. Miehe. Strain-driven homogenization of inelastic microstructures and composites based on an incremental variational formulation. *Int. J. Numer. Meth. Engrg.*, 55:1285–1322, 2002.
- [58] A. Mielke. Finite elastoplasticity, Lie groups and geodesics on $SL(d)$. In P. Newton, A. Weinstein, and P. J. Holmes, editors, *Geometry, Dynamics, and Mechanics*, pages 61–90. Springer-Verlag, New York, 2002.
- [59] A. Mielke. Evolution in rate-independent systems (Ch. 6). In C.M. Dafermos and E. Feireisl, editors, *Handbook of Differential Equations, Evolutionary Equations, vol. 2*, pages 461–559. Elsevier B.V., Amsterdam, 2005.
- [60] A. Mielke. Differential, energetic and metric formulations for rate-independent processes, pages 87–170. Springer, 2010.
- [61] A. Mielke and R. Rossi. Existence and uniqueness results for a class of rate-independent hysteresis problems. *Math. Models Meth. Appl. Sci.*, 17:81–123, 2007.
- [62] A. Mielke, R. Rossi, and G. Savaré. BV solutions and viscosity approximations of rate-independent systems. (Preprint no.1451, WIAS, Berlin). *ESAIM Control Optim. Calc. Var.*, 2010. in print.
- [63] A. Mielke and T. Roubíček. Rate-independent damage processes in nonlinear elasticity. *Math. Models Meth. Appl. Sci.*, 16:177–209, 2006.
- [64] A. Mielke and T. Roubíček. Numerical approaches to rate-independent processes and applications in inelasticity. *Math. Model. Numer. Anal.*, 43:399–428, 2009.
- [65] A. Mielke, T. Roubíček, and U. Stefanelli. Γ -limits and relaxations for rate-independent evolutionary problems. *Calc. Var., P.D.E.*, 31:387–416, 2008.
- [66] A. Mielke, T. Roubíček, and M. Thomas. From damage to delamination in nonlinearly elastic materials at small strains. *Journal of Elasticity*, 2010. submitted, WIAS Preprint 1542.
- [67] A. Mielke, T. Roubíček, and J. Zeman. Complete damage in elastic and viscoelastic media and its energetics. *Computer Methods Appl. Mech. Engrg.*, 199:1242–1253, 2010.
- [68] A. Mielke and F. Theil. A mathematical model for rate-independent phase transformations with hysteresis. In *Models of Continuum Mechanics in Analysis and Engineering* (H.-D. Alber, R.M.Balean, R.Farwig, Eds.), pages 117–129, Aachen, 1999. Shaker-Verlag.

- [69] A. Mielke and F. Theil. On rate-independent hysteresis models. *Nonl. Diff. Eqns. Appl. (NoDEA)*, 11:151–189, 2004. (Accepted July 2001).
- [70] A. Mielke, F. Theil, and V. I. Levitas. A variational formulation of rate-independent phase transformations using an extremum principle. *Arch. Rational Mech. Anal.*, 162:137–177, 2002.
- [71] A. Mielke and A.M. Timofte. Two-scale homogenization for evolutionary variational inequalities via the energetic formulation. *SIAM J. Math. Analysis*, 39:642–668, 2007.
- [72] M. Negri and C. Ortner. Quasi-static crack propagation by Griffith’s criterion. *Math. Models Methods Appl. Sci.*, 18:1895–1925, 2008.
- [73] M. Ortiz and E.A. Repetto. Nonconvex energy minimization and dislocation structures in ductile single crystals. *J. Mech. Phys. Solids*, 47:397–462, 1999.
- [74] M. Ortiz and L. Stainier. The variational formulation of viscoplastic constitutive updates. *Comput. Methods Appl. Mech. Engrg.*, 171:419–444, 1999.
- [75] H. Petryk. Incremental energy minimization in dissipative solids. *C. R. Mechanique*, 331:469–474, 2003.
- [76] N. Point. Unilateral contact with adherence. *Math. Methods Appl. Sci.*, 10:367–381, 1988.
- [77] N. Point and E. Sacco. A delamination model for laminated composites. *Math. Methods Appl. Sci.*, 33:483–509, 1996.
- [78] N. Point and E. Sacco. Mathematical properties of a delamination model. *Math. Comput. Modelling*, 28:359–371, 1998.
- [79] K.R. Rajagopal and A.R. Srinivasa. Mechanics of inelastic behavior of materials. part I and II. *Int. J. Plasticity*, 14:945–968, 969–998, 1998.
- [80] D. Rittel. Thermomechanical aspects of dynamic crack initiation. *Intl. J. Fracture*, 99:199–209, 1999.
- [81] R. Rossi and G. Savaré. Gradient flows of non convex functionals in Hilbert spaces and applications. *ESAIM Control Optim. Calc. Var.*, 12:564–614, 2006.
- [82] T. Roubíček. Rate independent processes in viscous solids at small strains. *Math. Methods Appl. Sci.*, 32:825–862, 2009. Erratum p. 2176.
- [83] T. Roubíček, V. Mantič, and C.G. Panagiotopoulos. Quasistatic mixed-mode delamination model. *Disc. Cont. Dynam. Syst. - S*, submitted.
- [84] T. Roubíček and R. Rossi. Adhesive contact delaminating at mixed mode, its thermodynamics and analysis. *in preparation*.
- [85] T. Roubíček and R. Rossi. Thermodynamics and analysis of rate-independent adhesive contact at small strains. *Nonlinear Anal., Th. Meth. Appl.*, 2011. in print.
- [86] T. Roubíček, L. Scardia, and C. Zanini. Quasistatic delamination problem. *Cont. Mech. Thermodynam.*, 21:223–235, 2009.
- [87] M. Shillor, M. Sofonea, and J.J. Telega. *Models and Analysis of Quasistatic Contact*. Springer, Berlin, 2004.
- [88] J.C. Simo. A framework for finite strain elastoplasticity based on maximum plastic dissipation and the multiplicative decomposition. *Comput. Methods Appl. Mech. Engrg.*, 66:199–219, 1988.
- [89] J.C. Simo and T.J.R. Hughes. *Computational Inelasticity*. Springer, New York, 1998.
- [90] M. Sofonea, W. Han, and M. Shillor. *Analysis and Approximation of Contact Problems and Adhesion or Damage*. Chapman & Hall, New York, 2006.
- [91] J. Svoboda and I. Turek. On diffusion-controlled evolution of closed solid-state thermodynamic systems at constant temperature and pressure. *Philosoph. Mag. B*, 64:749–759, 1991.
- [92] J.G. Swadener, K.M. Liechti, and A.L. deLozanne. The intrinsic toughness and adhesion mechanism of a glass/epoxy interface. *J. Mech. Phys. Solids*, 47:223–258, 1999.
- [93] L. Távara, V. Mantič, E. Graciani, J. Canas, and F. París. Analysis of a crack in a thin adhesive layer between orthotropic materials: an application to composite interlaminar fracture toughness test. *CMES*, 58:247–270, 2010.

- [94] L. Távara, V. Mantič, E. Graciani, and F. París. BEM analysis of crack onset and propagation along fiber-matrix interface under transverse tension using a linear elastic-brittle interface model. *Eng. Anal. Bound. Elem.*, 35:207–222, 2011.
- [95] M. Thomas. *Rate-independent damage processes in nonlinearly elastic materials*. PhD thesis, Institut für Mathematik, Humboldt-Universität zu Berlin, 2010.
- [96] M. Thomas and A. Mielke. Damage of nonlinearly elastic materials at small strain – Existence and regularity results –. *Z. angew. Math. Mech. (ZAMM)*, 90:88–112, 2010.
- [97] R. Toader and C. Zanini. An artificial viscosity approach to quasistatic crack growth. *Boll. Unione Matem. Ital.*, 2:1–36, 2009.
- [98] A. Turon, C.G. Davila, P.P. Camanho, and J. Costa. An engineering solution for mesh size effects in the simulation of delamination using cohesive zone models. *Eng. Fract. Mech.*, 74:1665–1682, 2007.
- [99] W. Tveergard and J.V. Hutchinson. The influence of plasticity on mixed mode interface toughness. *J. Mech. Physics Solids*, 41:1119–1135, 1993.
- [100] K. Uenishi and R. Rice. Universal nucleation length for slip-weakening rupture instability under nonuniform fault loading. *J. Geophys. Res.*, 108:1–14, 2003.
- [101] N. Valoroso and L. Champaney. A damage-mechanics-based approach for modelling decohesion in adhesively bonded assemblies. *Eng. Fract. Mech.*, 73:2774–2801, 2006.
- [102] Y. Wey and J.V. Hutchinson. Steady-state crack growth and work of fracture for solids characterized by strain gradient plasticity. *J. Mech. Phys. Solids*, 45:1253–1273, 1997.
- [103] D. Xie and A.M. Waas. Discrete cohesive zone model for mixed-mode fracture using finite element analysis. *Eng. Fract. Mech.*, 73:1783–1796, 2006.
- [104] H. Ziegler and Ch. Wehrli. On principle of maximum entropy rate production. *J. Non-Equil. Thermodynamic*, 12:229–243, 1987.

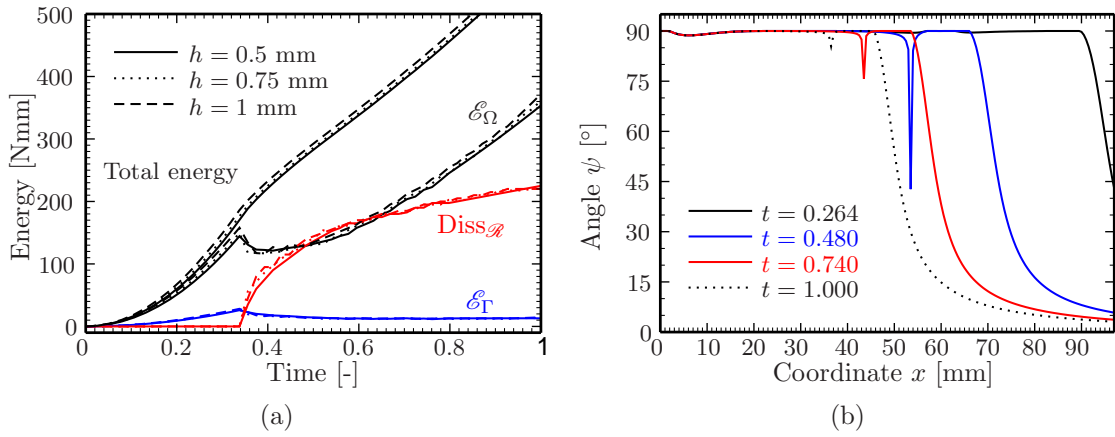


Figure 10:(a) Energetics of mixed mode flexure test (\mathcal{E}_Ω = energy stored in bulk, \mathcal{E}_Γ = interfacial contribution) and convergence for $h \rightarrow 0$, and (b) evolution of mixity-mode angles for $h = 0.5$ mm; $\tau = 0.025$.

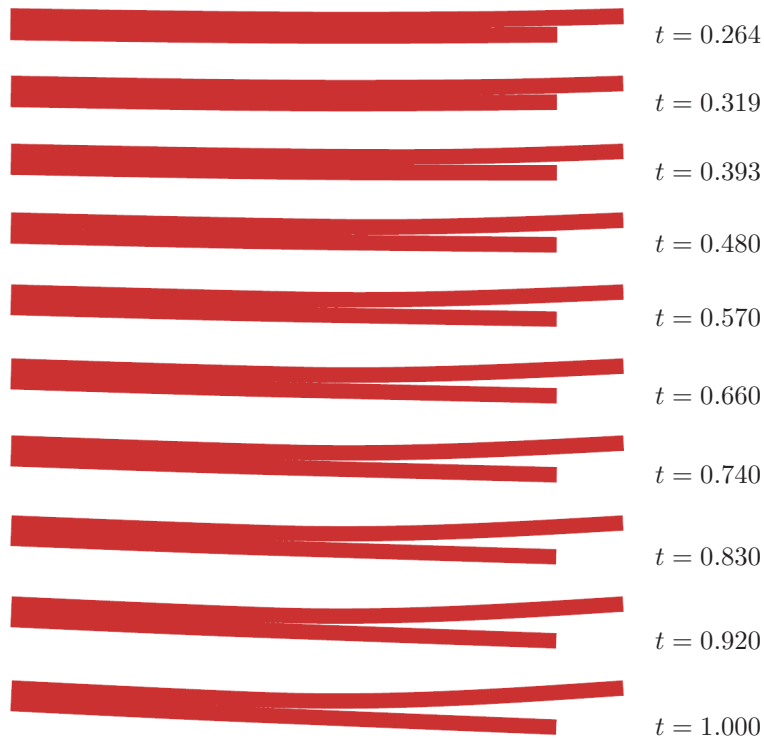


Figure 11:Ten snapshots of delamination evolution during the flexure test of a specimen from Figure 9; displacements depicted as magnified $5\times$.

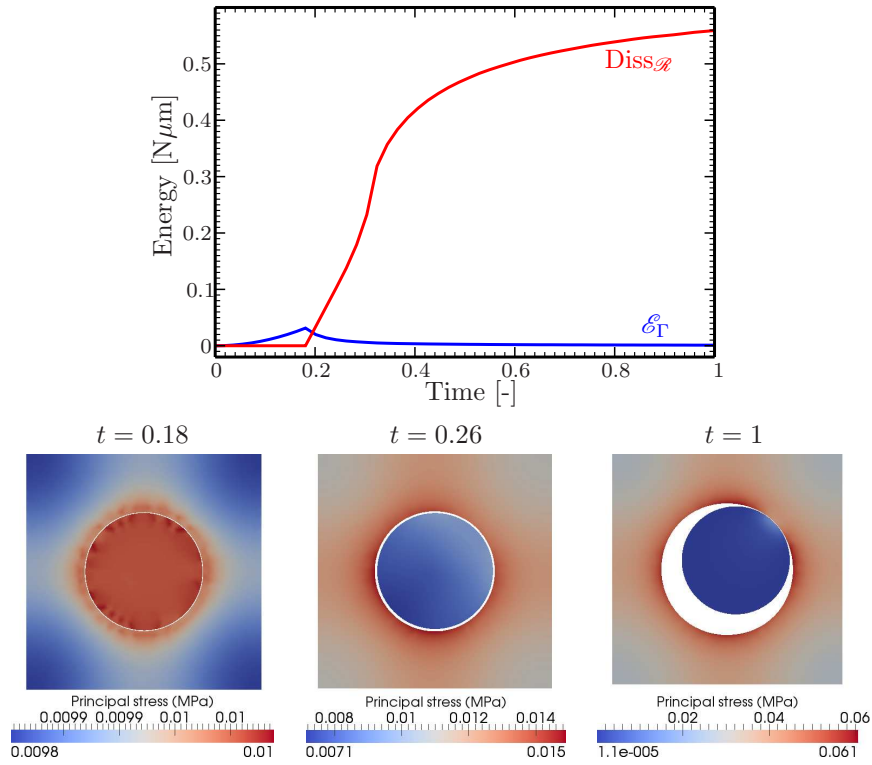


Figure 12: Energetics of a single-fiber debonding and three selected snapshots of displacement (depicted as magnified 20×) and spatial distribution of stress.

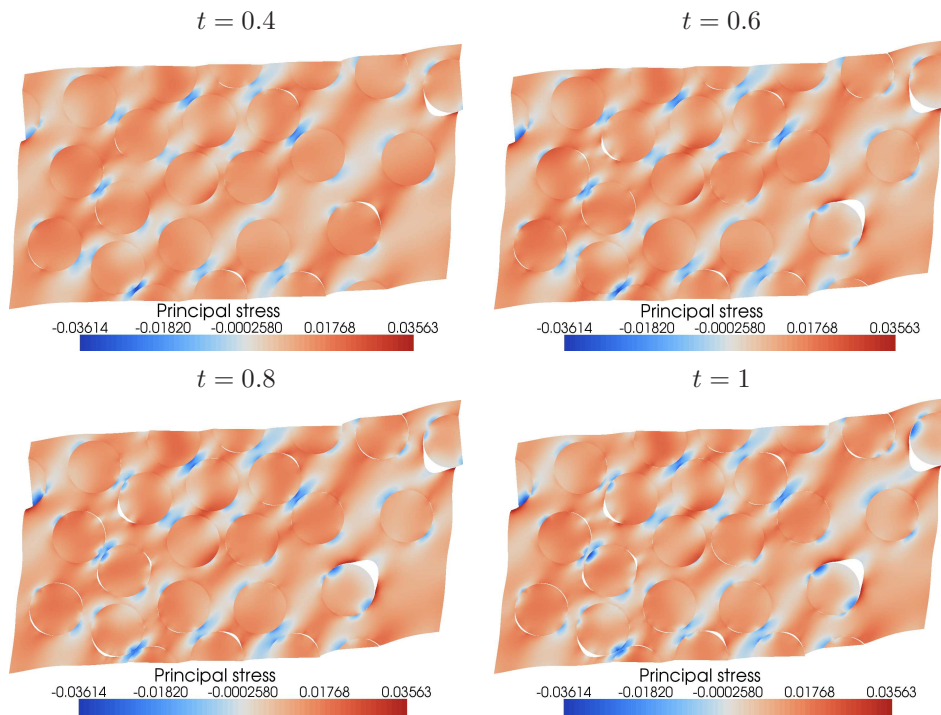


Figure 13: Debonding in a fiber-reinforced composite: 4 selected snapshots of a gradually loaded representative cell containing 20 fibers with depicted displacements (magnified 20×) and spatial distribution of stress.